

AD-A120 796

THERMODYNAMICS AND QUANTUM CORRECTIONS FROM MOLECULAR
DYNAMICS FOR LIQUID WATER(U) CALIFORNIA UNIV SAN DIEGO
LA JOLLA DEPT OF CHEMISTRY P H BERENS ET AL OCT 82

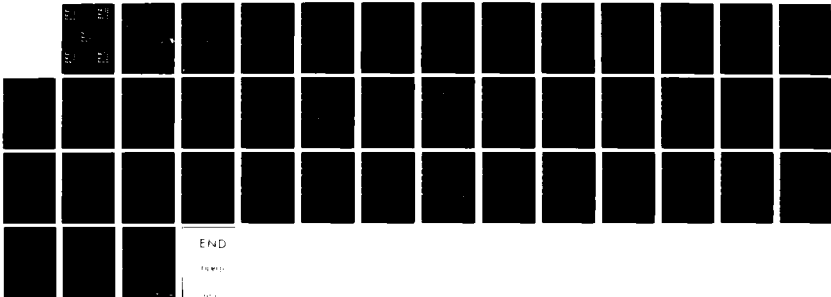
1/1

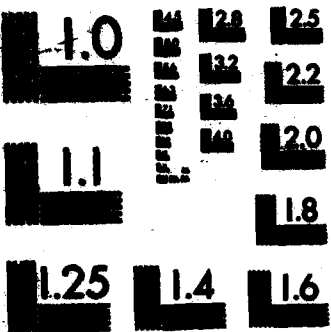
UNCLASSIFIED

TR-10 N00014-78-C-0325

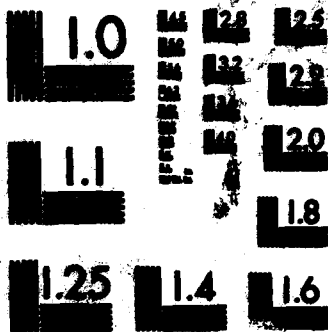
F/G 20/13

NL

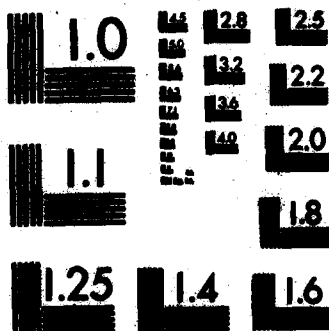




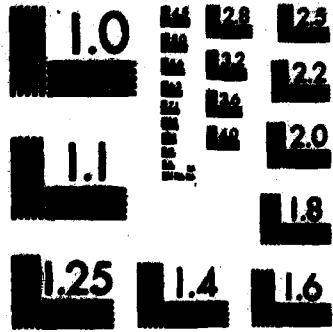
MICROCOPY RESOLUTION TEST CHART
NATIONAL BUREAU OF STANDARDS-1963-A



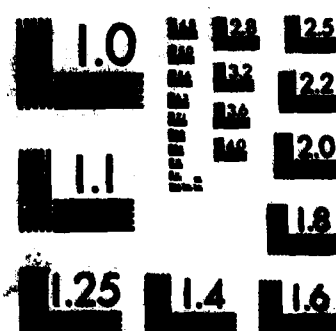
MICROCOPY RESOLUTION TEST CHART
NATIONAL BUREAU OF STANDARDS-1963-A



MICROCOPY RESOLUTION TEST CHART
NATIONAL BUREAU OF STANDARDS-1963-A



MICROCOPY RESOLUTION TEST CHART
NATIONAL BUREAU OF STANDARDS-1963-A



MICROCOPY RESOLUTION TEST CHART
NATIONAL BUREAU OF STANDARDS-1963-A

DA 120796

(3)

OFFICE OF NAVAL RESEARCH

Contract N00014-78 C-0325

TECHNICAL REPORT NO. 10

THERMODYNAMICS AND QUANTUM CORRECTIONS
FROM MOLECULAR DYNAMICS FOR LIQUID WATER

BY

Peter H. Berens, Donald H. J. Mackay, Gary M. White and
Kent R. Wilson

Department of Chemistry
University of California, San Diego
La Jolla, CA 92093

Prepared for Publication
in
The Journal of Chemical Physics

Reproduction in whole or in part is permitted for any purposes of the
United States Government.

This document has been approved for public release and sale; its distribution is unlimited.



DTIC FILE COPY

THERMODYNAMICS AND QUANTUM CORRECTIONS FROM MOLECULAR DYNAMICS FOR LIQUID WATER

Peter H. Berens, Donald H. J. Mackay, Gary M. White and Kent R. Wilson

Department of Chemistry
University of California, San Diego
La Jolla, CA 92093

ABSTRACT

In principle, given the potential energy function, the values of thermodynamic variables can be computed from statistical mechanics for a system of molecules. In practice for the liquid state, however, two barriers must be overcome. This paper treats the first problem, how to quantum correct the classical mechanical thermodynamic values available from molecular dynamics, Monte Carlo, perturbation, or integral methods in order to compare with experimental quantum reality. A subsequent paper will focus on the second difficulty, the effective computation of free energy and entropy. A simple technique, derived from spectral analysis of the atomic velocity time histories, is presented here for the quantum correction of classical thermodynamic values. This technique is based on the approximation that potential anharmonicities mainly affect the lower frequencies in the velocity spectrum where the system behaves essentially classically, while the higher spectral frequencies, where the deviation from classical mechanics is most pronounced, involve sufficiently harmonic atomic motions that harmonic quantum corrections apply. The approach is demonstrated by computation of the energy and constant volume heat capacity for water from classical molecular dynamics followed by quantum correction. The potential used to describe the interactions of the system of water molecules includes internal vibrational degrees of freedom and thus strong quantum effects. Comparison of the quantum corrected theoretical values with experimental measurements shows good agreement. The quantum corrections to classical thermodynamics (which are also derived for free energy and entropy) are shown to be important not only for internal vibrational motion, but also for intermolecular hindered rotational and translational motions in liquid water. They are presumably also important for other strongly associated molecules, including biomolecules, and thus should be included when comparing calculated and measured thermodynamic quantities. The approach illustrated here allows the calculation of thermodynamic quantum corrections for liquids, solutions, and large molecules such as polymers (including proteins and nucleic acids) with full inclusion of both intra- and intermolecular degrees of freedom.

Accession for
NTIS GEN&I
DTIC TAB
Unannounced
Justification

By _____
Distribution/
Availability Codes
Avail and/or
Dist Special

Submitted to *J. Chem. Phys.*, October 1982.



THERMODYNAMICS AND QUANTUM CORRECTIONS FROM MOLECULAR DYNAMICS FOR LIQUID WATER

Peter H. Berens, Donald H. J. Mackay, Gary M. White and Kent R. Wilson

Department of Chemistry
University of California, San Diego
La Jolla, CA 92093

I. INTRODUCTION

In principle from the potential energy as a function of nuclear positions one can compute from statistical mechanics the values of the thermodynamic variables. In practice this has been a difficult task for liquids and larger molecules such as proteins and nucleic acids. Two substantial barriers need to be overcome. The first, which is the subject of this paper, is how to compute quantum thermodynamic reality when only classical mechanics is practically available as a computational tool. That quantum mechanics is essential in treating intramolecular vibrations is universally acknowledged, but it has sometimes been less well appreciated that intermolecular motions in strongly associated liquids like water also show important quantum effects. Quantum corrections should thus be considered for strongly interacting molecules in general, even for molecules approximated as rigid bodies, and for biomolecules. The second barrier, which is the subject of a paper to follow, is how to practically compute the useful, but intrinsically difficult, free energy and entropy.

The present paper illustrates a simple molecular dynamics technique for quantum correcting classical thermodynamic quantities, for example those derived from molecular dynamics, Monte Carlo, perturbation, or integral methods. This approach makes use of the velocity spectrum (often called the velocity autocorrelation spectrum), which is related to infrared, Raman, and inelastic neutron spectra. For harmonic systems the velocity spectrum is directly linked to both classical and quantum mechanical thermodynamic parameters, as it then represents the density of normal mode harmonic oscillators as a function of frequency. Two suppositions are used to justify a harmonic approach to estimating the thermodynamic quantum corrections: 1) that anharmonicities mainly affect the low frequency motions which are nearly classical, and 2) that high frequency motions, where quantum effects are more important, are nearly harmonic. With these assumptions the quantum correction for a thermodynamic variable can be evaluated simply from the integral over frequency of a universal weighting function for that variable times the velocity spectrum computed from spectra of atomic velocity time histories. The weighting functions approach zero in the frequency region where anharmonicities would otherwise cause problems. Such a quantum correction approach is not limited, like most other approaches, to nearly classical systems, but can equally be used to treat molecular systems with internal vibrational degrees of freedom where quantum effects are very strong, for example molecular liquids, solutions, solids, and polymers, including proteins and nucleic acids, with full inclusion of internal degrees of freedom.

Section II describes the classical calculation of energy, heat capacity, free energy, and entropy from molecular dynamics, followed in Section III with the theory of our quantum correction technique. Section IV describes the calculation and quantum correction of the energy and heat capacity of liquid water. While quite good agreement is achieved with experiment, we emphasize that our main purpose is to illustrate the techniques and not to make the

PACS numbers: 03.65.Sq, 61.20.Ja, 61.25.Em, 82.60.Lf

The authors provided phototypeset copy for this paper using REFER.TBL; EQN; TROFF on UNIX.

most accurate possible thermodynamic calculations. We point out that the choice of boundary treatment can significantly affect the numerical results. Section V discusses these results and their meaning.

II. CLASSICAL THERMODYNAMICS FROM MOLECULAR DYNAMICS

The standard equations¹ linking the canonical partition function Q and the various thermodynamic variables are

$$E = k_B T^2 \frac{\partial \ln Q}{\partial T} \quad (2.1)$$

$$C_V = \frac{\partial E}{\partial T} \quad (2.2)$$

$$A = -k_B T \ln Q \quad (2.3)$$

$$S = k_B T \frac{\partial \ln Q}{\partial T} + k_B \ln Q, \quad (2.4)$$

in which E is the energy, C_V the constant volume heat capacity, A the Helmholtz free energy, S the entropy, k_B Boltzman's constant, and T the temperature.

A. Energy

The energy at a given temperature T may be computed from molecular dynamics in several ways. i) Choose initial conditions for a set of different constant energy microcanonical molecular dynamics runs to approximate a canonical ensemble at T , for example by a sequence of kinetic energy randomizations from a Boltzmann distribution. The classical energy of the system

$$E = \langle E_k(p^N) + V(r^N) \rangle, \quad (2.5)$$

is then derived as an average, symbolized by $\langle \rangle$, over several molecular dynamics runs from the ensemble at temperature T in which E_k is the kinetic energy and V the potential energy, letting the positions and momenta of the N atoms be represented by $r^N \equiv r_1, \dots, r_N$ and $p^N \equiv p_1, \dots, p_N$, respectively. ii) Compute the temperature for several different runs at different constant values of the total energy by averaging the instantaneous temperature defined in terms of the kinetic energy by

$$\langle T(t) \rangle = (3Nk_B)^{-1} \sum_{j=1}^{3N} m_j \langle [v_j(t)]^2 \rangle, \quad (2.6)$$

where k_B is Boltzman's constant, v_j is a Cartesian component of the velocity of one of the N atoms, m_j is the mass of that atom, and $\langle \rangle$ here indicates a time average. Fit an energy versus temperature curve to the results for several such microcanonical molecular dynamics runs. iii) Adjust the kinetic energies during each molecular dynamics run in order to represent the system in a heat bath at temperature T as demonstrated by Andersen.² In this paper we use both approaches i) and ii).

B. Heat capacity

By performing microcanonical molecular dynamics runs at several different energies and computing the average temperature for each energy, in other words method ii) above, the heat capacity at constant volume C_V can be derived through numerical differentiation of energy E with respect to the temperature T .

In addition, the heat capacity may be calculated in principle from the kinetic energy fluctuation for a microcanonical ensemble. With the velocity of the center of mass set to zero, the heat capacity is given by^{3,4}

$$C_V = R / \left[\frac{2}{3} - N \left(\frac{\langle T^2 \rangle - \langle T \rangle^2}{\langle T \rangle^2} \right) \right]. \quad (2.7)$$

in which R is k_B times Avogadro's number, the number of atoms is N , and T is defined as in Eq. (2.6) above. Statistical accuracy becomes very important as the denominator becomes small, which possibly explains why we did not succeed in calculating accurate values using this approach.

C. Free energy and entropy

The free energy may be computed from molecular dynamics by a technique due to Kirkwood^{1,5} which has been applied in a parallel manner to Monte Carlo calculations,⁶ as demonstrated by Mezei, Swaminathan and Beveridge^{7,8} in a classical Monte Carlo calculation of the free energy for rigid molecule liquid water.

The classical canonical ensemble partition function $Q(\xi)$ is defined as¹

$$Q(\xi) = (N!h^{3N})^{-1} \int \int dr^N dp^N \exp[-\beta H(r^N, p^N, \xi)], \quad (2.8)$$

in which $H(r^N, p^N, \xi)$ is the classical Hamiltonian of the system, the Kirkwood^{1,5-7} ξ is a parameter upon which the Hamiltonian depends, and $\beta \equiv (k_B T)^{-1}$. Eq. (2.3) now gives

$$A(\xi) = -\beta^{-1} \ln Q(\xi). \quad (2.9)$$

Differentiating Eq. (2.9) with respect to ξ gives

$$\frac{\partial A(\xi)}{\partial \xi} = -\beta^{-1} \frac{\partial \ln Q(\xi)}{\partial \xi} \quad (2.10)$$

which allows us to write

$$A(\xi_2) - A(\xi_1) = -\beta^{-1} \int_{\xi_1}^{\xi_2} d\xi \frac{\partial \ln Q(\xi)}{\partial \xi}, \quad (2.11)$$

in which ξ_2 is the value of the Kirkwood parameter which gives the real Hamiltonian and ξ_1 is a value which distorts the Hamiltonian to give a reference system (for example an ideal gas, a hard sphere liquid, or a harmonic solid) for which we can more easily compute the free energy.⁹ Using Eq. (2.8), we have

$$\begin{aligned} \frac{\partial \ln Q(\xi)}{\partial \xi} &= \frac{1}{Q(\xi)} \frac{\partial Q(\xi)}{\partial \xi} \\ &= -\beta(N!h^{3N})^{-1} \int \int dr^N dp^N \frac{\partial H(r^N, p^N, \xi)}{\partial \xi} \exp[-\beta H(r^N, p^N, \xi)] / Q(\xi) \end{aligned} \quad (2.12)$$

which by the ensemble postulate of Gibbs

$$= -\beta \langle \frac{\partial H(r^N, p^N, \xi)}{\partial \xi} \rangle_\xi, \quad (2.13)$$

where the derivative of the Hamiltonian with respect to ξ is averaged over coordinates and momenta from an ensemble with the Hamiltonian containing the parameter ξ . Substituting Eq. (2.13) into Eq. (2.11) gives

$$A(\xi_2) - A(\xi_1) = \int_{\xi_1}^{\xi_2} d\xi \langle \frac{\partial H(r^N, p^N, \xi)}{\partial \xi} \rangle_\xi. \quad (2.14)$$

To evaluate Eq. (2.14) by molecular dynamics, atomic trajectories are computed for the Hamiltonian $H(r^N, p^N, \xi)$. $\frac{\partial H(r^N, p^N, \xi)}{\partial \xi}$ is averaged over an ensemble of these trajectories at temperature T , and the result is then integrated between ξ_1 and ξ_2 .

In this way, the classical free energy change between the system with our real Hamiltonian $H(r^N, p^N, \xi)$ and a reference system with Hamiltonian $H(r^N, p^N, \xi_1)$ can be computed.

We chose the reference system to be one for which we can compute the classical free energy more tractably.

The entropy S of the system may then be calculated using

$$S = (E - A)/T. \quad (2.16)$$

We will illustrate in a subsequent paper the actual molecular dynamics calculation and quantum correction of the free energy and entropy of liquid water using approaches based on the Kirkwood technique.

III. QUANTUM CORRECTIONS FROM CLASSICAL MOLECULAR DYNAMICS

Outside of the trivial correction for vibrational zero point energy which may be calculated from spectroscopic data¹⁰ and which is generally introduced as a constant in the potential function, the vast majority of work in quantum corrections to classical thermodynamic computations stems from a method first introduced by Wigner¹¹ and Kirkwood.^{12, 13} In this approach the free energy is expanded in powers of \hbar^2 , and the first term in the quantum correction to be added to the classical value of the free energy is shown to be proportional to the classically averaged sum of the squares of the forces exerted on the particles in the system. The Wigner-Kirkwood technique has been modified, extended and tested by many workers.¹⁴⁻²² Others²³⁻³² have examined various methods to handle nondifferentiable potential functions which apply, for example, to hard spheres or square wells. Barker and Henderson have written a comprehensive review of liquids which includes an extensive section on quantum corrections.⁶

Another quantum correction method by Doll and Myers³³ is based on the path integral approach of Feynman and Hibbs.³⁴ It involves the calculation of an effective potential V_{eff} in the first stage of a Monte Carlo technique. In the second stage, V_{eff} is used to calculate the ratio between the quantum mechanical and classical partition functions. Stillinger³⁵ discusses the easier calculation of effective potentials for pairwise potentials.

In addition to the quantum corrections considered here there are the effects of the symmetry restrictions on quantum states imposed by Fermi-Dirac and Bose-Einstein statistics. In the temperature range of interest here these effects are negligible.^{12, 13, 36}

A disadvantage of all the previously cited techniques, except the vibrational zero point energy correction, is that they are ordinarily restricted to systems with small quantum effects. The method we present in this paper may be applied when quantum corrections are large, for example to intramolecular vibrations.

Öwicki and Scheraga³⁷ discuss the quantum corrections for liquid water. Using approximations to the effects of librational and vibrational frequencies, they calculate the quantum mechanical contributions from vibrational motion to energy and constant pressure heat capacity. These quantum contributions minus the classical values give their quantum corrections. They discuss the shift in the vibrational frequency of water as it enters the liquid phase which changes the zero point energy. This is necessary because they use rigid molecules. The type of nonrigid potential which we use includes both intra- and intermolecular degrees of freedom and thus in principle (but not yet in practice due to potential energy function inaccuracies as is discussed below) can take into account the frequency changes from gas to liquid.

The quantum correction technique used in the present paper involves calculating the velocity spectrum $S(\nu)$ from molecular dynamics and then integrating $S(\nu)$ over all frequencies with a weighting function which is the difference between the quantum and classical harmonic weighting functions for the thermodynamic variable of interest.

A. Velocity spectrum

The velocity spectrum $S(\nu)$ of a classical system of N atoms in equilibrium is defined as

$$S(\nu) = 4\pi\beta \sum_{j=1}^{1V} m_j \langle D[v_j(\nu)] \rangle. \quad (3.1)$$

in which ν is frequency, $\beta = (k_B T)^{-1}$ in which k_B is Boltzman's constant and T is the temperature, m_j is the mass of the atom corresponding to the j th Cartesian velocity component as a function of time $v_j(t)$, and $\langle \rangle$ indicates an average over the ensemble. The spectral density operator D (for which windowing and window correction techniques are described elsewhere^{38, 39}) is evaluated in terms of probability per unit angular frequency,

$$D[v_j(t)] \equiv (2\pi)^{-1} \lim_{T \rightarrow \infty} \frac{1}{2T} \left| \int_{-T}^T dt \exp(-i2\pi\nu t) v_j(t) \right|^2. \quad (3.2)$$

The velocity spectrum may also be computed from the Fourier transform of the velocity auto-correlation function. Note that the velocity spectrum can be computed separately for different subsets of atoms (for example, different elements, different chemical environments of the same element, or different molecules) and the velocity spectrum $S(\nu)$ can then be computed as a sum of the effects from these different subsets of atoms. Thus, as we will see, the quantum corrections also can be partitioned among the different subsets of atoms. Even though once the dynamics, i.e. the set of velocities $\{v_j(t)\}$, is determined, the quantum corrections may be computed separately for different subsets of atoms, it should be remembered that normally all atoms together contribute to determining the dynamics.

It will be useful below to know the value of the integral $\int_0^\infty d\nu S(\nu)$. The Fourier transform of a real function, e.g. $v_j(t)$, has an even real part and an odd imaginary part.⁴⁰ The square of the absolute value of such a Fourier transform, e.g. $D[v_j(t)]$, is a real even function. A linear combination of real even functions, e.g. $S(\nu)$, is also a real even function. Therefore $S(-\nu) = S(\nu)$ which allows us to write

$$\int_0^\infty d\nu S(\nu) = \int_{-\infty}^\infty d\nu S(\nu)/2. \quad (3.3)$$

Substituting Eq. (3.2) into Eq. (3.1) and inserting the result into the right side of Eq. (3.3) gives

$$\int_0^\infty d\nu S(\nu) = \beta \int_{-\infty}^\infty d\nu \sum_{j=1}^{3N} m_j \langle \lim_{T \rightarrow \infty} \frac{1}{2T} \left| \int_{-T}^T dt \exp(-i2\pi\nu t) v_j(t) \right|^2 \rangle. \quad (3.4)$$

Let

$$v_j^r(t) = \begin{cases} v_j(t) & \text{if } -\tau < t < \tau \\ 0 & \text{otherwise,} \end{cases} \quad (3.5)$$

and let the Fourier transform of $v_j^r(t)$ be $F_j^r(\nu)$, i.e.,

$$F_j^r(\nu) = \int_{-\infty}^\infty dt \exp(-i2\pi\nu t) v_j^r(t) = \int_{-\tau}^\tau dt \exp(-i2\pi\nu t) v_j(t). \quad (3.6)$$

Substituting Eq. (3.6) into Eq. (3.4) gives

$$\int_0^\infty d\nu S(\nu) = \beta \int_{-\infty}^\infty d\nu \sum_{j=1}^{3N} m_j \langle \lim_{T \rightarrow \infty} \frac{1}{2T} \left| F_j^r(\nu) \right|^2 \rangle. \quad (3.7)$$

Exchanging integration and the $T \rightarrow \infty$ limit gives

$$\int_0^\infty d\nu S(\nu) = \beta \sum_{j=1}^{3N} m_j \langle \lim_{T \rightarrow \infty} \frac{1}{2T} \int_{-\tau}^\tau d\nu \left| F_j^r(\nu) \right|^2 \rangle. \quad (3.8)$$

By Parseval's theorem,⁴⁰

$$\int_{-\infty}^\infty d\nu \left| F_j^r(\nu) \right|^2 = \int_{-\infty}^\infty dt \left| v_j^r(t) \right|^2 = \int_{-\tau}^\tau dt \left| v_j(t) \right|^2 = \int_{-\tau}^\tau dt \left(v_j(t) \right)^2 \quad (3.9)$$

since $v_j(t)$ is a real function. Substituting Eq. (3.9) into Eq. (3.8) gives

$$\int_0^\infty d\nu S(\nu) = \beta \sum_{j=1}^{3N} m_j \left\langle \lim_{\tau \rightarrow \infty} \frac{1}{2\tau} \int_{-\tau}^{\tau} dt \left(v_j(t) \right)^2 \right\rangle \quad (3.10)$$

$$= 2\beta \sum_{j=1}^{3N} \left\langle \lim_{\tau \rightarrow \infty} \frac{1}{2\tau} \int_{-\tau}^{\tau} dt \frac{m_j}{2} \left(v_j(t) \right)^2 \right\rangle. \quad (3.11)$$

Since by classical equipartition of energy¹

$$\langle E_k \rangle = \sum_{i=1}^{3N} \lim_{\tau \rightarrow \infty} \frac{1}{2\tau} \int_{-\tau}^{\tau} dt \frac{m_i}{2} \left(v_i(t) \right)^2 = \frac{3N}{2\beta} \quad (3.12)$$

in which $\langle E_k \rangle$ is the average kinetic energy,

$$\int_0^\infty d\nu S(\nu) = 2\beta \left(3N/2\beta \right) = 3N, \quad (3.13)$$

i.e. the integral of the velocity spectrum from zero to infinite frequency is just three times the number of atoms, which will be true for any potential, harmonic or not. This relation can be used as a check on the accuracy of computation of $S(\nu)$, and to interpret $S(\nu)$ in terms of an equivalent density of normal modes even for anharmonic systems.

The diffusion coefficient has a particularly simple expression in terms of the velocity spectrum. The diffusion coefficient \bar{D} of a particle with position history $r(t)$ is defined as⁴¹

$$\bar{D} = \frac{1}{3} \lim_{\tau \rightarrow \infty} \frac{1}{2\tau} \langle [r(\tau) - r(0)]^2 \rangle \quad (3.14)$$

where $\langle \cdot \rangle$ indicates an ensemble average. Letting the three Cartesian components of $r(t)$ be $x(t)$, $y(t)$ and $z(t)$, we have

$$\bar{D} = \frac{1}{3} \lim_{\tau \rightarrow \infty} \frac{1}{2\tau} \langle [x(\tau) - x(0)]^2 + [y(\tau) - y(0)]^2 + [z(\tau) - z(0)]^2 \rangle. \quad (3.15)$$

For isotropic systems, the equation may be simplified to

$$\bar{D} = \lim_{\tau \rightarrow \infty} \frac{1}{2\tau} \langle [x(\tau) - x(0)]^2 \rangle, \quad (3.16)$$

or

$$\bar{D} = \frac{1}{2} \lim_{\tau \rightarrow \infty} \frac{1}{2\tau} \langle [x(\tau) - x(-\tau)]^2 \rangle, \quad (3.17)$$

where $x(\tau)$ now represents any one of the three Cartesian components of $r(\tau)$. If we let $D_0[v_j(t)]$ denote the value of the spectral density at zero frequency, then Eq. (3.2) becomes

$$D_0[v_j(t)] = (2\pi)^{-1} \lim_{\tau \rightarrow \infty} \frac{1}{2\tau} [x(\tau) - x(-\tau)]^2. \quad (3.18)$$

Combining Eqs. (3.17) and (3.18) we get

$$\bar{D} = \pi \langle D_0[v_j(t)] \rangle. \quad (3.19)$$

If $S(\nu)$ is restricted to equivalent particles, then Eq. (3.1) becomes

$$S(\nu) = 4\pi\beta m \sum_{j=1}^{3M} \langle D[v_j(t)] \rangle = 12\pi M m \beta \langle D[v_j(t)] \rangle \quad (3.20)$$

where M particles are being considered each of mass m . Then

$$\langle D_0[v_j(t)] \rangle = S(0)/12\pi M m \beta \quad (3.21)$$

and thus the diffusion constant \bar{D} is related to the zero frequency value of the velocity spectrum $S(0)$ by

$$\bar{D} = S(0)/12Mm\beta, \quad (3.22)$$

in which M is the number of equivalent particles, m is their mass, and $\beta = (k_B T)^{-1}$ in which k_B is Boltzman's constant and T is the temperature. The most usual application of Eq. (3.22) is to consider the particles to be molecules and to compute the diffusion constant from the zero frequency value of the velocity spectrum of the center of mass of the molecules.

B. Harmonic approximation

We quantum correct the classical thermodynamic variables using a harmonic oscillator approximation. This correction is based on a division of the dynamics in frequency space. The low frequency region is viewed as nearly classical but containing the major anharmonic effects, and the high frequency region is viewed as nearly harmonic and thus can be quantum corrected exactly within the limits of the harmonic approximation.

Consider a system of N atoms as linked by harmonic potentials.

$$V(\mathbf{r}^N) = V_0 + \frac{1}{2} \sum_{j,k=1}^{3N} \frac{\partial^2 V}{\partial r_j \partial r_k} \Delta r_j \Delta r_k \quad (3.23)$$

in which Δr_j and Δr_k are displacements from a potential minimum and V_0 is the potential energy at that minimum. Such a harmonic situation can be approached classically in the limit of small atomic motions about a potential minimum, i.e. at low temperatures, but one should remember that quantum wave functions sample the potential in a region about the minimum even at absolute zero, and thus anharmonicity, both explicit and due to coupling by finite displacements, will always play a role in real systems. Nonetheless, we believe that at higher frequencies an analysis which uses the finite temperature classical velocity spectrum interpreted as if it were fully harmonic will usually sufficiently well represent the thermodynamic quantum corrections.

In the harmonic limit, a normal mode analysis allows us to view the system as a set of $3N$ harmonic oscillators with q_j as a single oscillator partition function. The total canonical partition function Q for the system can then be expressed in terms of the partition functions q_j for the individual modes as

$$Q = \prod_{j=1}^{3N} q_j \quad (3.24)$$

or

$$\ln Q = \sum_{j=1}^{3N} \ln q_j. \quad (3.25)$$

If the normal frequencies are continuously distributed we may take the integral

$$\ln Q = \int_0^\infty d\nu S(\nu) \ln q(\nu) \quad (3.26)$$

where $S(\nu)$ is the density of normal modes with frequency ν .

To show that the velocity spectrum of a system of particles linked through harmonic potentials represents the density of normal modes, the $3N$ time varying Cartesian position components, x_1, \dots, x_{3N} , are first represented in terms of normal coordinates. We have⁴²

$$x_k = (m_k)^{-\frac{1}{2}} \sum_{j=1}^{3N} a_{jk} q_j \quad (3.27)$$

$$q_j = A_j \sin(\omega_j t + \theta_j) \quad (3.28)$$

where q_1, \dots, q_{3N} are the normal coordinates, $\omega_1, \dots, \omega_{3N}$ are the characteristic normal mode angular frequencies in which $2\pi\nu_j = \omega_j$, A_j is the j th normal mode amplitude, θ_j is its phase, and a_{jk} are constants scaled such that

$$\sum_{k=1}^N \omega_k^2 = 1. \quad (3.29)$$

The kinetic and potential energies in terms of the normal coordinates a_j , which have units of length times square root of mass and \dot{a}_j , which are the time derivatives, are

$$E_k = \frac{1}{2} \sum_{j=1}^N \dot{a}_j^2 \quad (3.30)$$

$$V = \frac{1}{2} \sum_{j=1}^N \omega_j^2 a_j^2. \quad (3.31)$$

From Eqs. (3.27) and (3.30) we have

$$x_k = (m_k)^{-\frac{1}{2}} \sum_{j=1}^N a_j A_j \sin(\omega_j t + \theta_j) \quad (3.32)$$

$$v_k = \dot{x}_k = (m_k)^{-\frac{1}{2}} \sum_{j=1}^N a_j \omega_j A_j \cos(\omega_j t + \theta_j). \quad (3.33)$$

Inserting Eq. (3.33) into Eq. (3.1) we get

$$\langle E_k \rangle = \langle m_k \dot{x}_k^2 \rangle = m_k \left\langle \left(\sum_{j=1}^N a_j \omega_j A_j \cos(\omega_j t + \theta_j) \right)^2 \right\rangle. \quad (3.34)$$

$$= m_k \sum_{j=1}^N \langle a_j^2 \omega_j^2 A_j^2 \cos^2(\omega_j t + \theta_j) \rangle. \quad (3.35)$$

Applying this to Eq. (3.30) gives

$$\langle E_k \rangle = m_k \sum_{j=1}^N \langle a_j^2 \omega_j^2 \rangle / 2 = m_k \left[\langle (\omega_j + \omega_i)^2 + 2(\omega - \omega_i) \rangle \right] / 2. \quad (3.36)$$

$$= m_k \sum_{j=1}^N [\delta(\omega_j + \omega_i) \delta(\omega + \omega_i) + \delta(\omega - \omega_i)] \quad (3.37)$$

where Eq. (3.29) has been used.

Applying the theory of composition of energy to Eq. (3.36) we get

$$\langle E \rangle^{-1} = \langle v^2/2 \rangle \quad (3.38)$$

$$= \langle \omega/4 \rangle \cos^2(\omega t + \theta)/2 \quad (3.39)$$

$$= \omega/4. \quad (3.40)$$

in which $\langle \cdot \rangle$ here denotes a time average. Substituting this into Eq. (3.37) gives as our final result

$$S(v) = 2\pi \sum_{j=1}^N \delta(\omega_j + \omega) + \delta(\omega - \omega_j) = \sum_{j=1}^N \delta(\omega + \omega_j) + \delta(\omega - \omega_j). \quad (3.40)$$

This, then, the velocity spectrum, which is computed from the Cartesian velocity time histories, is indeed the normal mode density for a harmonic system.

C. Classical weighting functions

The classical partition function for a single harmonic oscillator (normalized as usual to the quantum partition function by the inclusion of \hbar^{-1}) is¹

$$g_C^*(v) = (\beta h\nu)^{-1} = u^{-1} \quad (3.41)$$

at ¹ The symbol C indicates that the variable is derived classically. $u = \beta h\nu$ is the

reduced energy of the harmonic oscillator, $\beta = (k_B T)^{-1}$, h is Planck's constant and ν is the frequency of the oscillator. Substituting Eq. (3.41) into Eq. (3.26), and inserting this result into Eqs. (2.1) through (2.4) gives

$$E^C = V_0 + k_B T \int_0^\infty d\nu S(\nu) W_E^C(\nu); \quad W_E^C(\nu) = 1 \quad (3.42)$$

$$C_v^C = k_B \int_0^\infty d\nu S(\nu) W_{C_v}^C(\nu); \quad W_{C_v}^C(\nu) = 1 \quad (3.43)$$

$$A^C = V_0 + k_B T \int_0^\infty d\nu S(\nu) W_A^C(\nu); \quad W_A^C(\nu) = \ln u \quad (3.44)$$

$$S^C = k_B \int_0^\infty d\nu S(\nu) W_S^C(\nu); \quad W_S^C(\nu) = [1 - \ln u]. \quad (3.45)$$

These classical weighting functions $W^C(\nu)$ are shown in Fig. 1. To allow the zero of energy to be set arbitrarily, we include V_0 , the energy of the system treated classically if all oscillations are stilled. The expressions for energy and heat capacity reduce to the familiar classical results

$$E^C = V_0 + 3Nk_B T \quad (3.46)$$

$$C_v^C = 3Nk_B. \quad (3.47)$$

D. Quantum weighting functions

The quantum mechanical partition function for a single harmonic oscillator is¹

$$q^Q(\nu) = \frac{e^{-u/2}}{1 - e^{-u}} \quad (3.48)$$

where the superscript Q indicates that the variable is derived quantum mechanically and again $u \equiv \beta h\nu$ is the reduced energy. Substituting Eq. (3.48) into Eq. (3.26) and inserting this result into Eqs. (2.1) through (2.4) gives

$$E^Q = V_0 + k_B T \int_0^\infty d\nu S(\nu) W_E^Q(\nu); \quad W_E^Q(\nu) = \left(\frac{u}{2} + \frac{u}{e^u - 1} \right) \quad (3.49)$$

$$C_v^Q = k_B \int_0^\infty d\nu S(\nu) W_{C_v}^Q(\nu); \quad W_{C_v}^Q(\nu) = \left(\frac{u^2 e^u}{(1 - e^u)^2} \right) \quad (3.50)$$

$$A^Q = V_0 + k_B T \int_0^\infty d\nu S(\nu) W_A^Q(\nu); \quad W_A^Q(\nu) = \left[\ln \frac{1 - e^{-u}}{e^{-u/2}} \right] \quad (3.51)$$

$$S^Q = k_B \int_0^\infty d\nu S(\nu) W_S^Q(\nu); \quad W_S^Q(\nu) = \left[\frac{u}{e^u - 1} - \ln(1 - e^{-u}) \right]. \quad (3.52)$$

Fig. 1 shows these quantum weighting functions $W^Q(\nu)$.

For a system which closely approximates a set of harmonic oscillators, such as a perfect crystal at low temperature,^{1,9} the above equations alone can be used to compute the thermodynamic variables.

E. Quantum correction weighting functions

The quantum corrections (indicated by the superscript Δ) are obtained by subtracting the classical representations from the quantum mechanical representations for the given thermodynamic variable.

$$W^\Delta(\nu) = W^Q(\nu) - W^C(\nu) \quad (3.53)$$

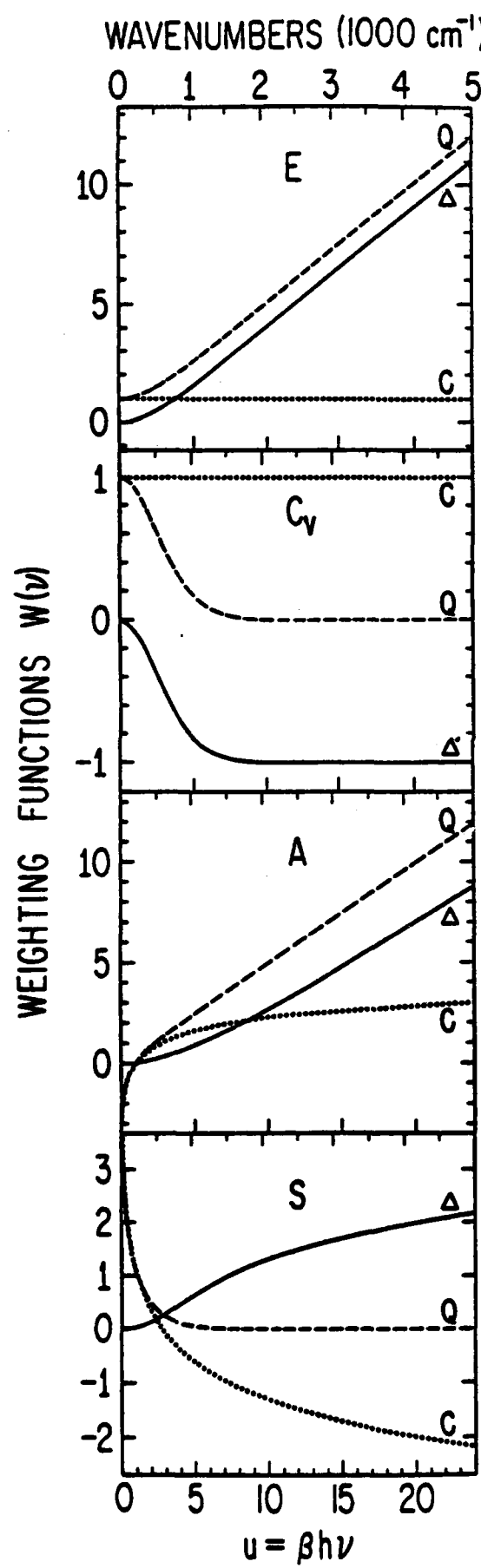


FIG. 1. Universal harmonic weighting functions $W(\nu)$ for the thermodynamic functions of any harmonic system. Dotted lines are classical $W^C(\nu)$ from Eqs. (3.42) to (3.45), dashed lines are quantum $W^Q(\nu)$, from Eqs. (3.49) to (3.52), and solid lines are quantum correction $W^\Delta(\nu) = W^Q(\nu) - W^C(\nu)$, from Eqs. (3.54) to (3.57). It is thus the solid line curves which are used to weight the velocity spectra $S(\nu)$ to compute the quantum corrections to the thermodynamic functions. The top panel is for energy E , the next to the top panel is for constant volume heat capacity C_v , the next to the bottom panel is for Helmholtz free energy A , and the bottom panel is for entropy S . The lower horizontal scale is plotted in reduced energy $u = \beta h\nu$ in which $\beta = k_B T$, k_B being Boltzman's constant and T the temperature, while h is Planck's constant and ν the frequency of the oscillator. The upper horizontal scale is the wavenumber equivalent to u at 300 K. Note that all the quantum correction weighting functions go to zero at low frequency where anharmonic effects become important.

$$E^\Delta = E^Q - E^C = k_B T \int_0^\infty d\nu S(\nu) W_E^\Delta(\nu); \quad W_E^\Delta(\nu) = \left[\frac{u}{2} + \frac{u}{e^u - 1} - 1 \right] \quad (3.54)$$

$$C_v^\Delta = C_v^Q - C_v^C = k_B \int_0^\infty d\nu S(\nu) W_{C_v}^\Delta(\nu); \quad W_{C_v}^\Delta(\nu) = \left[\frac{u^2 e^u}{(1 - e^u)^2} - 1 \right] \quad (3.55)$$

$$A^\Delta = A^Q - A^C = k_B T \int_0^\infty d\nu S(\nu) W_A^\Delta(\nu); \quad W_A^\Delta(\nu) = \left[\ln \frac{1 - e^{-u}}{e^{-u/2}} - \ln u \right] \quad (3.56)$$

$$S^\Delta = S^Q - S^C = k_B \int_0^\infty d\nu S(\nu) W_S^\Delta(\nu); \quad W_S^\Delta(\nu) = \left[\frac{u}{e^u - 1} - \ln(1 - e^{-u}) + \ln u - 1 \right]. \quad (3.57)$$

The quantum correction weighting functions $W^\Delta(\nu)$ are also shown in Fig. 1. Note that following Eqs. (3.1), (3.2), and (3.54)-(3.57) we can partition if we wish the quantum corrections among different subsets of atoms, for example different elements, different chemical environments of the same element, different molecules, or molecules in different environments.

IV. MOLECULAR DYNAMICS RESULTS FOR LIQUID WATER

Water is the most important of all solvents, and the molecular level understanding of its bulk properties is of considerable intrinsic interest. We have thus chosen it as a test case for our techniques. A quantum calculation for a system of molecules large enough to adequately represent liquid water is at present impractical, and thus thermodynamic quantities are computed by classical mechanics, usually by Monte Carlo or molecular dynamics techniques. Such classical molecular mechanics calculations on liquid water have been discussed in reviews by Stillinger,³⁵ Barnes,⁴⁴ Wood,⁴⁵ and Beveridge et al.⁴⁶ Goel and Hockney⁴⁷ have written a comprehensive bibliography for earlier molecular dynamics in general. It will be shown for liquid water that quantum corrections are needed for both inter and intramolecular motions to match experimental quantum reality.

A. Liquid water potentials and previous computer simulations

A major obstacle for any molecular mechanics computer simulation is the development of an accurate potential surface. Both experimental data and quantum calculations are valuable to this end. Bernal and Fowler⁴⁸ (BF) in 1933 have given a rigid three point charge plus Lennard-Jones potential for water. An empirical potential for water was introduced in 1951 by Rowlinson⁴⁹ (ROW), and tested by Barker and Watts.⁵⁰⁻⁵² This is a rigid four point charge model with a Lennard-Jones oxygen-oxygen potential. The analytical form of the Rowlinson potential has been utilized in several improved potentials, namely BNS and ST2. Ben-Naim and Stillinger introduced the BNS potential⁵³ in 1972, and Rahman and Stillinger⁵⁴⁻⁵⁶ and others⁵² utilized it in several test studies. After finding the potential too tetrahedronally directional⁵⁵ and noting an improvement after an energy rescaling⁵⁴ Stillinger and Rahman introduced the ST2 potential⁵⁷ in 1974. ST2 has been used and tested extensively by many workers.⁵⁸⁻⁶⁷

Shipman and Scheraga⁶⁸ have developed a seven point charge effective pair potential (SS) for water using a variety of experimental data. Both water dimer⁶⁹ and ice-like water cluster⁷⁰ studies have been carried out. In an attempt to include intramolecular vibrations, to allow for possible molecular dissociation,⁵⁶ and to account for some of the nonadditive interaction⁷¹ between waters, Lemberg and Stillinger introduced a central force potential¹⁹ (LS) in 1975. In this scheme both bonded and nonbonded oxygen-hydrogen interactions use the same potential as do all hydrogen-hydrogen interactions. It has been both further applied⁷² and improved⁷³ (LS2).

An *ab initio* water potential prepared by fitting analytical functions to quantum mechanically calculated energy versus nuclear position data was developed by Popkie, Kistenmacher and Clementi⁷⁴ in 1973 at the Hartree-Fock level. Several studies⁷⁵⁻⁸⁰ have used this potential

(HF), and it has been found that the neglect of electron correlation effects leads to significant inaccuracies.^{75, 77, 78} In response, Matsuoka, Clementi and Yoshimine⁸¹ carried out *ab initio* calculations with configuration interaction to account for correlation effects. The resulting potential (CI) has been tested by several investigators.^{63, 67, 82-87} A specific comparison of the HF and CI potentials has been carried out by Swaminathan and Beveridge.⁸⁸ The CI potential has been criticized because of lack of agreement with experimental liquid density,³⁷ its poor reproduction of the second virial coefficient of steam⁸³ and the high rms error in fitting the original calculations.⁸⁹

Watts has provided a flexible water dimer potential⁹⁰ (WATTS) in which a largely empirical intermolecular potential is complemented by an intramolecular potential derived from vibrational spectroscopy. The WATTS potential has been studied and criticized by McDonald and Klein.^{89, 91}

Several more recent water potentials deserve mention. Stillinger and David⁹² have developed a polarization potential (SD) in order to describe deformable water molecules and Stillinger⁹³ has studied its dynamic properties. The importance of non pairwise additive effects for water is also stressed by Barnes et al.,⁹⁴ and they introduce a polarizable electropole model (PE) and test it in a water-amino acid system.⁹⁵ Goodfellow⁹⁶ continues this study of cooperative effects and the PE potential by showing how the PE model can be efficiently applied. The present parameterization of the PE model has been criticized recently because the oxygen-oxygen radial distribution agrees poorly with experiment.⁴⁶ Nemenoff, Snir, and Scheraga⁹⁷ have developed an empirical technique (EPEN/2) for potential function development which has been revised by Marchese, Mehrotra and Beveridge.⁹⁸ Berendsen et al.⁹⁹ have produced a single point charge (SPC) potential with Lennard-Jones interaction between oxygens in order to handle conveniently protein-water systems. Jorgensen has developed a set of transferable intermolecular potential functions (TIPS) for application to organic liquids and water.¹⁰⁰ Reimers, Watts, and Klein¹⁰¹ propose a revised version (RWK2) of the WATTS potential.

Many molecular dynamic^{54, 57, 59-61, 64, 72, 86, 87, 91, 102} calculations have been carried out as well as Monte Carlo^{7, 8, 37, 46, 50-52, 62-65, 67, 74, 75, 78, 82, 84, 85, 100, 101, 103, 104} calculations on liquid water using most of the potentials described above. In addition, Weress and Rice¹⁰⁵ discuss the calculation of liquid water thermodynamic properties and their quantum corrections using the BNS potential (with some modifications) and a cell model viewpoint.

Several papers have tested and compared the variety of water-water potentials, often with disappointing results. Morse and Rice¹⁰⁶ calculate some of the properties of ice with many of the above potentials. The results raise serious questions about the ability of ST2, WATTS, and LS2 to accurately reproduce the properties of ice while CI, with the exception of reproducing too low densities, fares well. Reimers and Watts¹⁰¹ make a related comparison extending to all three phases. WATTS, ROW, and BNS reproduce the second virial coefficient of steam well but fail in the other two phases. CI and ST2 do well for the liquid phase but fail with ice and steam. They conclude that all models tested are generally inadequate to handle all three phases, but that their revised RWK2 potential fares best.

B. Molecular dynamics

Our molecular dynamics calculations are carried out on a system of 250 water molecules at a density of 1.0 g cm^{-3} and a temperature of 300 K with cubic periodic boundary conditions using a special molecular mechanics package running on an array processor.^{107, 108} Experimentally, this density corresponds to a pressure of 85 atm with a negligible resulting difference¹⁰⁹ of $0.012 \text{ kJ mole}^{-1}$ in total energy compared to a pressure of 1 atm which corresponds to a density of 0.997 g cm^{-3} . Previous molecular dynamics calculations of thermodynamic quantities for water have been carried out using an array processor by Rapaport and Scheraga^{87, 110} who studied a sample of 343 rigid waters using the CI potential with long runs and by Swope, Andersen, Berens, and Wilson¹⁰² who studied the properties of water clusters. The software used previously^{107, 108} has been augmented by an intermolecular force and energy calculator for water as implemented by Swope and Andersen.¹¹¹ This calculator utilizes a piecewise fifth order

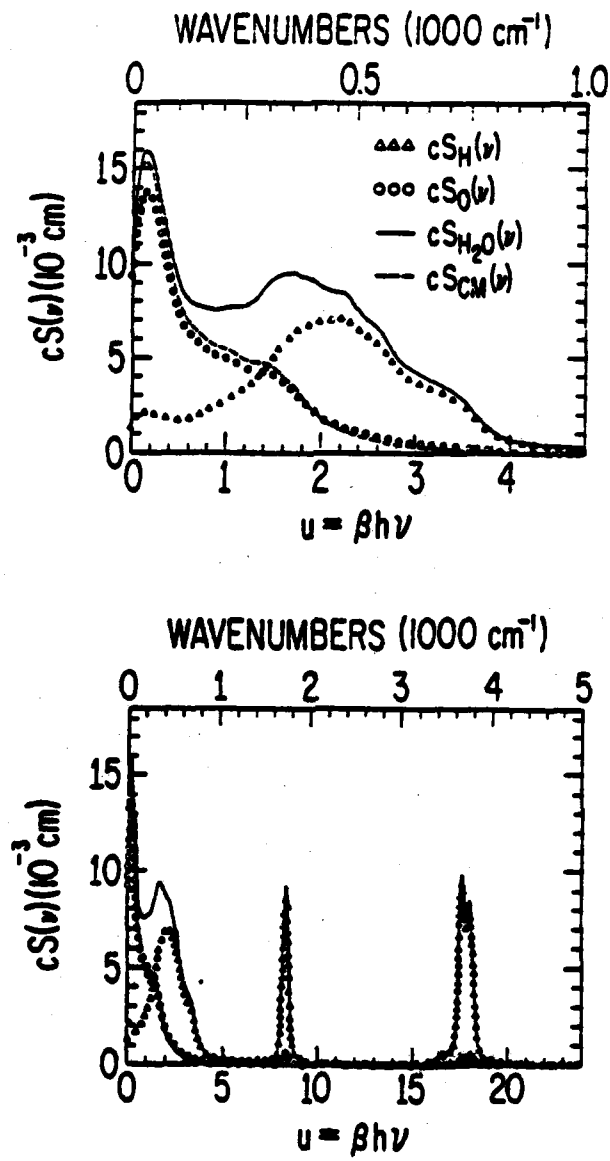


FIG. 2. Velocity spectra times the speed of light c normalized for one molecule of H_2O at 300 K and 1.0 g cm^{-3} , using the Watts potential with 250 waters and cubic periodic boundary conditions. The lower panel contains $cS_H(\nu)$ for the hydrogen atoms per molecule of water, $cS_O(\nu)$ for the oxygen atoms per molecule of water, the sum, $cS_H(\nu) + cS_O(\nu) = cS_{H_2O}(\nu)$, and the center of mass velocity spectrum $cS_{CM}(\nu)$. The upper panel is a blowup of the low frequency region of the lower panel. The lower horizontal scales are in terms of the reduced energy $u = \beta h\nu$ in which $\beta = (k_B T)^{-1}$ and ν is the frequency. The speed of light c is included so that the integral of $cS(\nu)$ in cm vs the upper scale of wavenumbers in cm^{-1} will be dimensionless, giving the total number of equivalent harmonic oscillators. For a purely harmonic system the velocity spectrum $S(\nu)$ would give the number of harmonic modes per unit frequency. Note that the H atoms dominate $S_{H_2O}(\nu)$ above 300 cm^{-1} and the O atoms below it.

polynomial fitted to the analytical potential energy functions as a function of the square of the distance between the two atoms being considered. It thus both allows a general algorithm to evaluate the polynomial previously fitted to arbitrary analytic functions and eliminates the necessity of a square root operation.

The method for applying a switching function as developed by Andersen and Swope smooths each water-water energy contribution to zero as the corresponding oxygen-oxygen distance passes through the switching region, which for our system extended from 0.85 to 0.90 nm. This technique eliminates the problem of artificially created monopoles (and possibly large dipoles) normally encountered by an atom-atom force feathering or truncation method as only part of the water molecule passes through the feathering region (and is possibly imaged). This artifact is especially pronounced with water unless the Andersen-Swope technique is used, as the partial charges on each atom are relatively large.

The semiempirical flexible water molecule potential developed by Watts⁹⁰ is used. The intramolecular potential is a standard Taylor's series in internal coordinates about the potential minimum as derived from vibrational spectroscopy. The intermolecular potential is pairwise by atoms and fitted to the second virial coefficient of steam.

Equilibration of the initial water system is accomplished by following periods of dynamics (0.1 - 2.0 picoseconds) with randomizations of velocity according to a Maxwell-Boltzmann distribution at the desired temperature until the temperature of the system stabilizes. The total simulation time involved in equilibration is approximately 60 picoseconds. The time step of integration during equilibration is 0.5 femtoseconds while for the data collection a time step of 0.25 femtoseconds is used.

The velocity data is accumulated by selecting out the velocities every 12 time steps over a period of 50 000 time steps (12.3 picoseconds total simulation time). A more elegant approach would be to use a digital low-pass filter before sampling.¹¹² The energy and heat capacity data are the result of a much longer series of seven runs for a total of 380 000 time steps over 95 picoseconds.

C. Velocity spectra

The velocity spectra $S(\nu)$ shown in Fig. 2 are calculated by fast Fourier transforms of the velocity time histories of various components of the system. We define the following normalized velocity spectra

$$S_H(\nu) = \frac{4\pi\beta}{M} \sum_{j=1}^M m_j^H \langle D[v_j^H(t)] \rangle \quad (4.1)$$

$$S_O(\nu) = \frac{4\pi\beta}{M} \sum_{j=1}^M m_j^O \langle D[v_j^O(t)] \rangle \quad (4.2)$$

$$S_{H_2O}(\nu) = S_O(\nu) + S_H(\nu) \quad (4.3)$$

$$S_{CM}(\nu) = \frac{4\pi\beta}{M} \sum_{j=1}^M m_j^{H_2O} \langle D[v_j^{CM}(t)] \rangle \quad (4.4)$$

where m^O , m^H , and m^{H_2O} represent the masses of an oxygen atom, hydrogen atom, and water molecule respectively; D is the spectral density operator defined in Eq. (3.2); $v_j^O(t)$, $v_j^H(t)$ and $v_j^{CM}(t)$, represent the velocity time histories of the j th oxygen atom, hydrogen atom and molecular center of mass respectively; M is the number of water molecules, where $M \equiv N/3$; and a factor of $1/M$ has been introduced to normalize the velocity spectra to that for one molecule of water. The contribution to $S_{H_2O}(\nu)$ by both the oxygens and the hydrogens is determined by computing each spectrum, $S_O(\nu)$ and $S_H(\nu)$, separately. The high frequency vibrational peaks composed mainly of the oxygen-hydrogen vibrations are easily seen in Fig. 2. The center of mass velocity spectrum of the system is also computed and its spectrum reflects the highly damped vibrational modes of whole water molecules.

The area under $S_{H_2O}(\nu)$ in Fig. 2 equals 9.0, the equivalent number of harmonic oscillators (including hindered translation and rotation) per molecule of water, as expected from Eq. (3.13). (The speed of light is introduced to make the integral versus cm^{-1} unitless.) The double peak in the range $2600\text{--}5000 \text{ cm}^{-1}$ which corresponds to the symmetric and asymmetric stretching modes of the water molecule has an area of 1.89. The peak in the range $1200\text{--}2600 \text{ cm}^{-1}$ which corresponds to the bending of the HOH bond angle has an area of 1.00. This substantiates the view of $S(\nu)$ as a density of normal modes and further suggests that the close association of the water molecules in the liquid phase has shifted some of the high frequency stretching motion down into the low frequency region.

In principle a potential with both intra and intermolecular degrees of freedom like the WATTS potential we have used could take into account the frequency changes from gas to liquid. The actual frequencies for the WATTS potential for the gas phase should be close to the harmonic values¹¹³ of $\nu_1 = 3832 \text{ cm}^{-1}$ (symmetric stretch), $\nu_2 = 1649 \text{ cm}^{-1}$ (bend), and $\nu_3 = 3943 \text{ cm}^{-1}$ (asymmetric stretch), compared to the computed liquid phase peaks centered at 3680, 1740, and 3760 cm^{-1} as shown in Fig. 2. In real water, the infrared and Raman spectra show the gas phase anharmonic frequencies¹¹⁴ to be 3652, 1595, and 3756 cm^{-1} and the liquid phase^{10, 115} shows a bending peak at approximately 1650 cm^{-1} and a broad stretching peak centered at approximately 3400 cm^{-1} with perhaps a subsidiary peak at approximately 3200 cm^{-1} . Thus the WATTS vibrational shifts from gas to liquid phase qualitatively resemble the real water shifts with large shifts downward in frequency for the stretching motions and a smaller shift upward for the bending motion, but the agreement is certainly not quantitative.

From $S_{CM}(0)$ in Fig. 2 and Eq. (3.22) we obtain for the center of mass diffusion coefficient \bar{D} of water a value of $4.08 \times 10^{-9} \text{ m}^2\text{s}^{-1}$ compared to the experimental value^{116, 117} of $2.42 \times 10^{-9} \text{ m}^2\text{s}^{-1}$ for liquid water at 300 K. The precision of our reported value is questionable because we selected out every twelfth velocity rather than all velocities for the fast Fourier transform due to computer memory limitations, and a more reliable value could be computed from the asymptotic slope of the mean square displacement of the center of mass for a long molecular dynamics run. It should also be remembered that the finite size of the periodic boundaries may affect the longest wavelength and lowest frequency motions and in particular that hydrodynamic or concerted motions involving many molecules may not be accurately handled.

Berendsen et al.¹¹⁸ have reported a spectral density of the center of mass of rigid molecule liquid water, using the previously described SPC potential, which is strikingly similar to our $S_{CM}(\nu)$. They report a diffusion coefficient of $3.6 \times 10^{-9} \text{ m}^2\text{s}^{-1}$.

D. Quantum corrections

The difference between the classical and quantum mechanical weighting functions $W(\nu)$ arises from the difference between the classical and quantum harmonic oscillator partition functions $q(\nu)$. In the classical limit of $\hbar \rightarrow 0$, or equivalently $u \rightarrow 0$, $\nu \rightarrow 0$, or $T \rightarrow \infty$, this distinction disappears,

$$\lim_{\hbar \rightarrow 0} q^Q(\nu) = \lim_{\hbar \rightarrow 0} q^C(\nu). \quad (4.5)$$

This implies

$$\lim_{\hbar \rightarrow 0} W^Q(\nu) = \lim_{\hbar \rightarrow 0} W^Q(\nu) = \lim_{\hbar \rightarrow 0} W^C(\nu) \quad (4.6)$$

and thus,

$$W^A(0) = W^Q(0) - W^C(0) = 0 \quad (4.7)$$

in all cases, as can be seen in Fig. 1. The divergence of $W^Q(\nu)$ from $W^C(\nu)$ as ν increases results in a preferential weighting of high frequency motions in the calculation of quantum corrections.

Table I gives the liquid water quantum corrections computed from the velocity spectrum $S_{H_2O}(\nu)$ from Eqs. (4.1) to (4.3) as shown in Fig. 2 and the quantum correction weighting functions $W^A(\nu)$ as shown in Fig. 1, using Eqs. (3.54) to (3.57). The curves of the products of $S(\nu)$ and W^A for energy, heat capacity, free energy and entropy are shown in Figs. 3 to 6, illustrating the contribution to the quantum corrections as a function of frequency and of atom type. A separation is made for the purposes of Table I in frequency space at 1200 cm^{-1} between the intermolecular and intramolecular motions for liquid water. Note that the intermolecular motions, the hindered translation and rotation, contribute substantially to the total quantum corrections.

TABLE I. Inter- and intramolecular contributions to liquid water quantum corrections at 300 K, per mole.

	Inter (0-1200 cm^{-1})	Intra (1200-5000 cm^{-1})	Total
$E^\Delta(\text{kJ})$	4.2	45.0	49.2
$C_v^\Delta(\text{J/K})$	-11.0	-23.8	-34.8
$A^\Delta(\text{kJ})$	2.2	33.4	35.6
$S^\Delta(\text{J/K})$	6.5	38.8	45.3

Classically, a harmonic oscillator contributes $k_B T$ to the energy regardless of frequency as a result of equipartition of energy. This produces a straight line for the classical weighting function in the top panel of Fig. 1. Quantum mechanics, however, requires that a harmonic oscillator contain a minimum or zero point energy of $\hbar\nu/2$. For a harmonic oscillator with $\hbar\nu \ll k_B T$, this requirement is unimportant and quantum effects are small. In contrast, a quantum harmonic oscillator with $\hbar\nu \gg k_B T$ has an average energy near $\hbar\nu/2$. As a result

$$\lim_{\nu \rightarrow \infty} W_E^Q(\nu) = u/2 = \beta \frac{\hbar\nu}{2}. \quad (4.8)$$

Thus the quantum effects are large for a high frequency harmonic oscillator as it contributes $\hbar\nu/2$ to the energy instead of $k_B T$. Table I shows a value of 49.2 kJ for the total quantum correction to energy. Others have accounted for this quantum effect by introducing a constant into the potential energy function. Using spectroscopic data, Eisenberg and Kauzmann¹⁰ have calculated 55.45 kJ as a zero point energy.

Heat capacity is unique in that it results in a negative quantum correction, and it has the most significant contribution from the low frequency region compared to the other corrections we have listed. As a result of equipartition of energy, the classical harmonic oscillator contributes k_B to C_v regardless of frequency. This produces a straight line in the next to the top panel of Fig. 1. In contrast, the quantum mechanical harmonic oscillator with $\hbar\nu \gg k_B T$ is "stuck" in the ground state and changes very little in response to changes in temperature. As a result,

$$\lim_{\nu \rightarrow \infty} W_{C_v}^Q(\nu) = 0. \quad (4.9)$$

Thus, for each harmonic oscillator with $\hbar\nu \gg k_B T$, k_B must be subtracted from the classically calculated C_v . The importance of the low frequency contribution to the quantum correction for constant volume heat capacity results from the rapid divergence of $W_{C_v}^Q(\nu)$ and $W_{C_v}^C(\nu)$ as ν increases from zero.

The equation $A = E - TS$ holds in an analogous manner for the quantum corrections as a result of the linear form of the quantum correction equations. The energy term dominates for harmonic oscillators and thus the quantum correction for free energy is always positive.

The reader may be surprised that the quantum correction for entropy is positive. A quantum mechanical harmonic oscillator with $\hbar\nu \gg k_B T$ is stuck in the ground state and

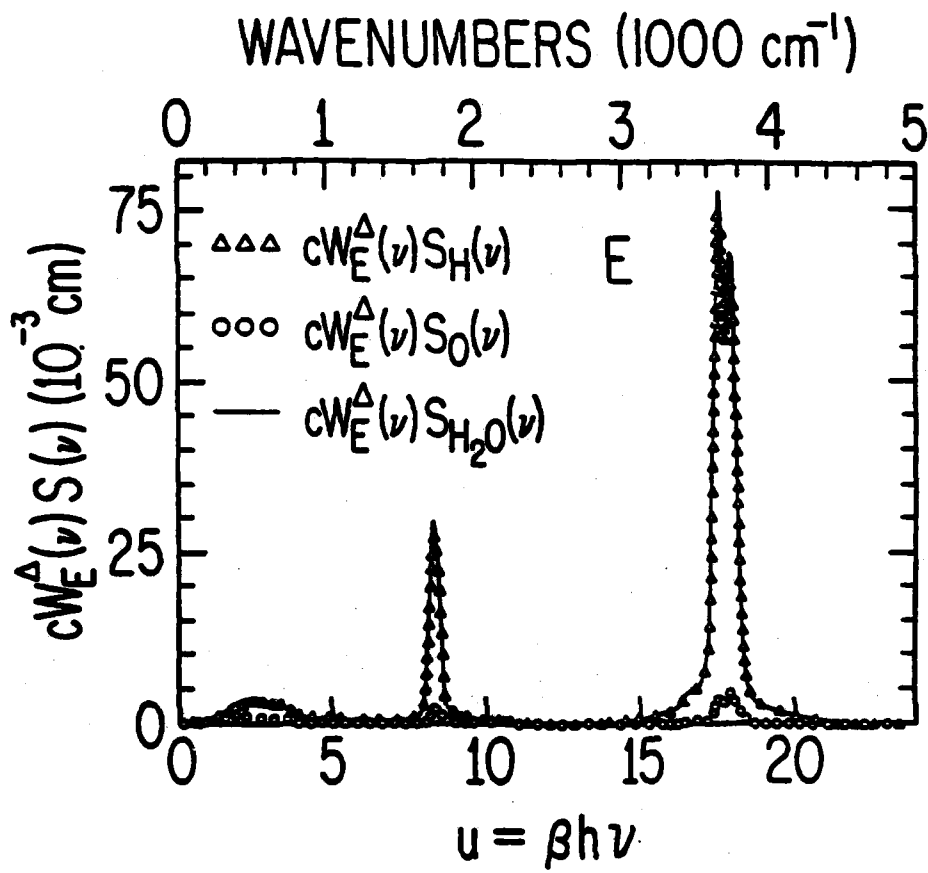


FIG. 3. Energy quantum correction curves for liquid water for H atoms, for O atoms, and their sum giving the total H_2O . Plotted is the product of the speed of light c , the velocity spectrum $S(\nu)$, and the energy quantum correction weighting function $W_E^{\Delta}(\nu)$ vs the reduced oscillator energy $u = \beta h \nu$ on the bottom axis and the wavenumber equivalent at 300 K on the top axis. The integral of the product $S(\nu) W_E^{\Delta}(\nu)$ vs ν gives the quantum correction to energy, as shown in Eq. (3.54). The Figure also illustrates how the quantum correction partitions between the O atoms and the H atoms which dominate at all but the lowest frequencies.

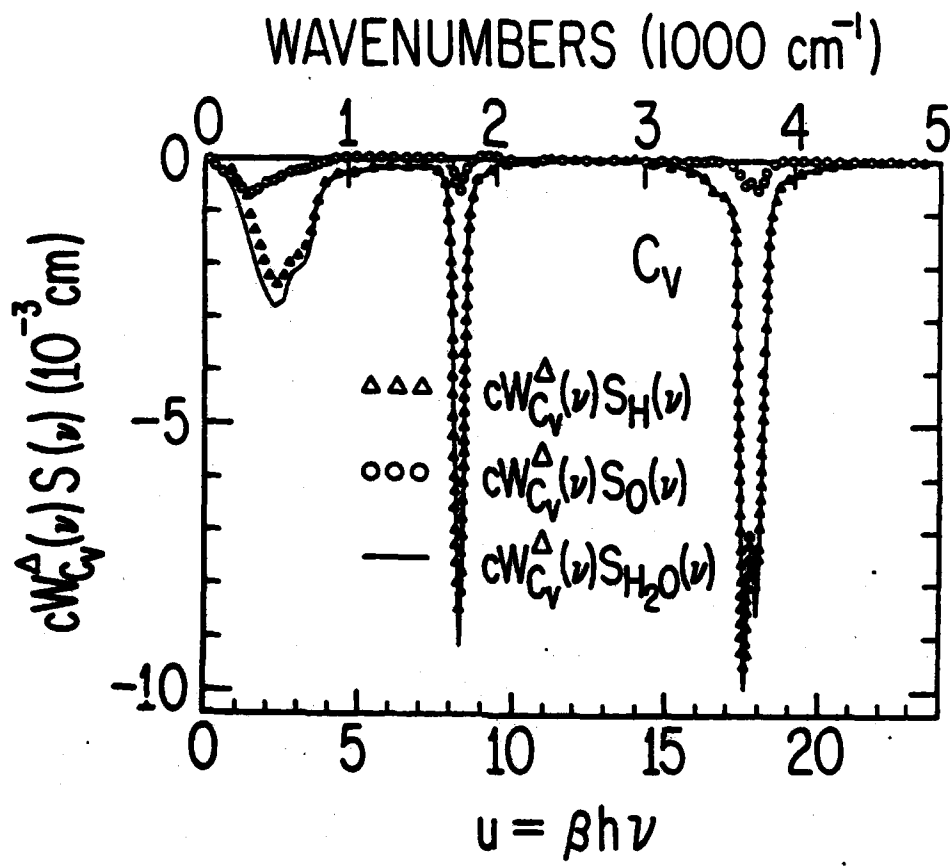


FIG. 4. Constant volume heat capacity quantum correction curves for liquid water for H atoms, for O atoms, and their sum giving the total H_2O quantum correction. Plotted is the product of the speed of light c , the velocity spectrum $S(\nu)$, and the heat capacity quantum correction weighting function $W_{C_V}^\Delta(\nu)$ vs the reduced oscillator energy $u = \beta h\nu$ on the bottom axis and the wavenumber equivalent at 300 K on the top axis. The integral of the product $S(\nu) W_{C_V}^\Delta(\nu)$ vs ν gives the quantum correction to constant volume heat capacity, as shown in Eq. (3.55).

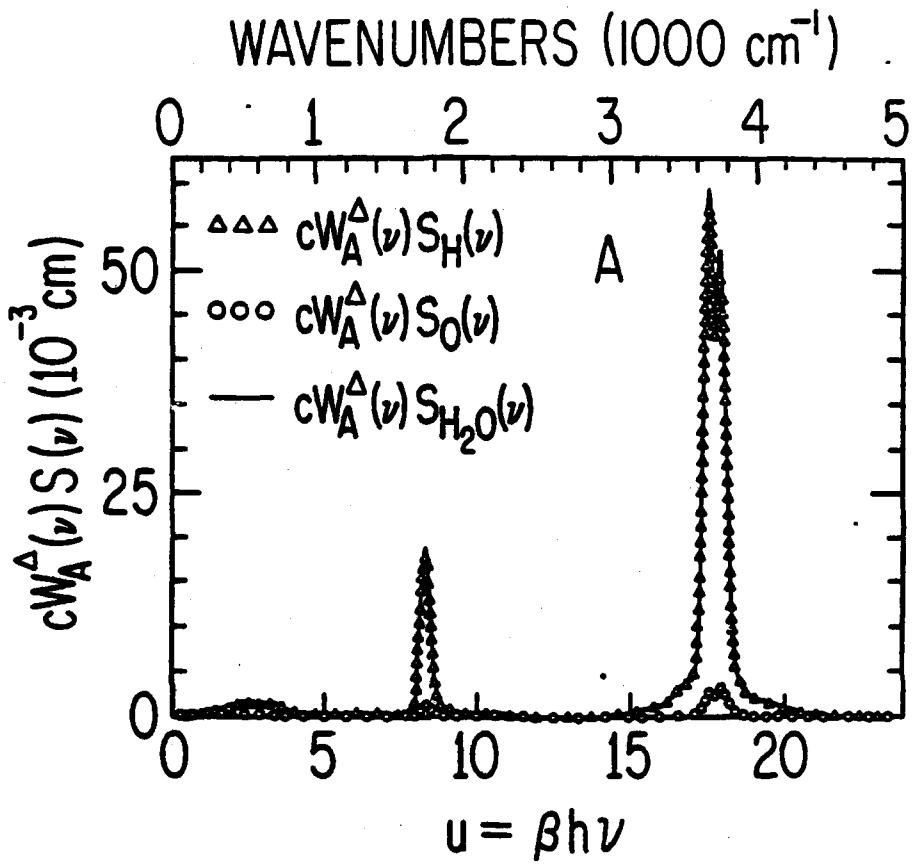


FIG. 5. Helmholtz free energy quantum correction curves for liquid water for H atoms, for O atoms, and their sum giving the total H_2O quantum correction. Plotted is the product of the speed of light c , the velocity spectrum $S(\nu)$, and the Helmholtz free energy quantum correction weighting function $W_A^\Delta(\nu)$ vs the reduced oscillator energy $u = \beta h\nu$ on the bottom axis and the wavenumber equivalent at 300 K on the top axis. The integral of the product $S(\nu) W_A^\Delta(\nu)$ vs ν gives the quantum correction to Helmholtz free energy, as shown in Eq. (3.56).

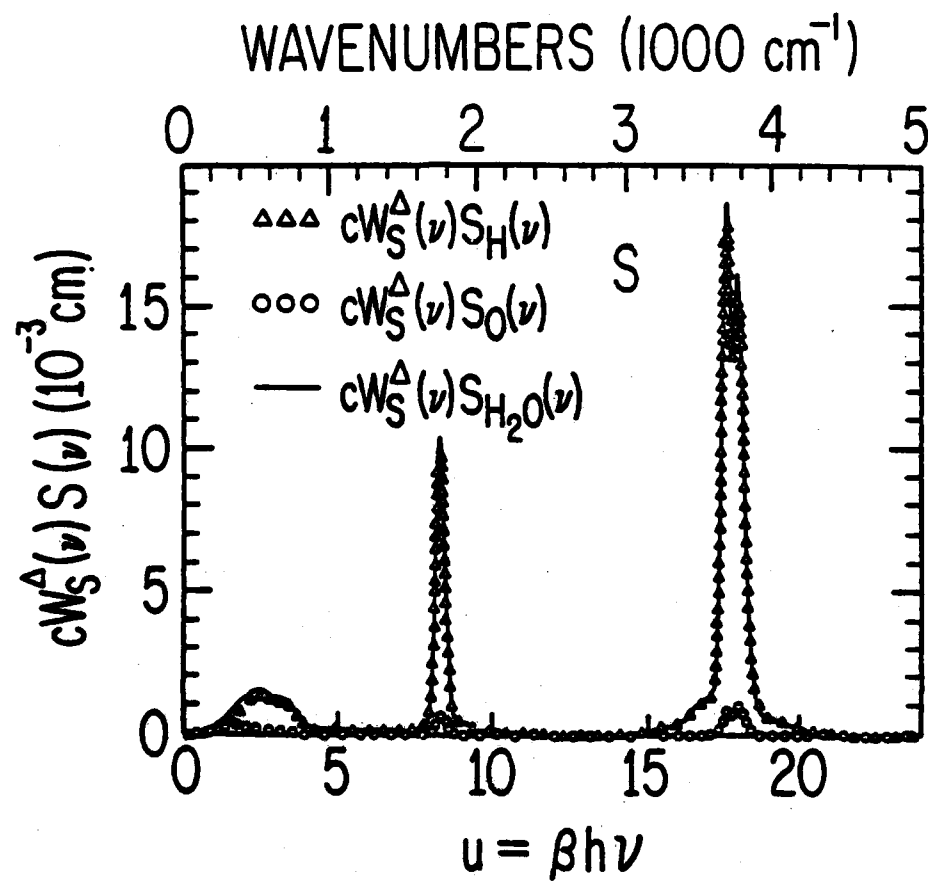


FIG. 6. Entropy quantum correction curves for liquid water for H atoms, for O atoms, and their sum giving the total H_2O quantum correction. Plotted is the product of the speed of light c , the velocity spectrum $S(\nu)$, and the entropy quantum correction weighting function $W_s^\Delta(\nu)$ vs the reduced oscillator energy $u \equiv \beta h\nu$ on the bottom axis and the wavenumber equivalent at 300 K on the top axis. The integral of the product $S(\nu) W_s^\Delta(\nu)$ vs ν gives the quantum correction to entropy, as shown in Eq. (3.57).

contributes almost nothing to the entropy. Thus, as seen in Fig. 1,

$$\lim_{\nu \rightarrow \infty} W_S^Q(\nu) = 0. \quad (4.10)$$

In contrast, the classical harmonic oscillator weighting function has the following properties.

$$\lim_{\nu \rightarrow 0} W_S^C(\nu) = \infty. \quad (4.11)$$

$$\lim_{\nu \rightarrow \infty} W_S^C(\nu) = -\infty. \quad (4.12)$$

The first equation indicates that an unconstrained particle has an unlimited number of available states. The second equation results from the difficulty of applying the third law of thermodynamics to the classical representation of entropy for a harmonic oscillator. Because of the negative sign of the classical weighting function, the quantum correction for entropy is positive.

Figures 3 to 6 show the products of the velocity spectra $S(\nu)$ with the quantum correction weighting functions $W^A(\nu)$ for energy E , constant volume heat capacity C_V , Helmholtz free energy A , and entropy S . Since $S_{H_2O}(\nu)$ can be partitioned into separate contributions from the hydrogen and oxygen atoms, we also partition the products $S_{H_2O}(\nu) W^A(\nu)$ and thus compute separately the hydrogen and oxygen atom contributions to the quantum corrections. The hydrogen atom motions dominate except at the very lowest frequencies which have little weight anyway.

E. Energy

Seven water samples with different energies are created and equilibrated, and the average temperature for each sample, calculated over at least ten picoseconds running time, is plotted in Fig. 7. A straight line is fitted to the points, and the total classical energy E^C corresponding to 300 K is calculated. By averaging over a subset (500 time steps selected over a time period of 1.25 picoseconds) of a complete run at 300 K we also compute the average value of the intramolecular potential energy V_{intra} ; the intermolecular potential energy V_{inter} ; and the kinetic energy E_k as shown in Table II. Because E^C is calculated from the fitting shown in Fig. 7 while V_{intra} , V_{inter} , and E_k are calculated from the short subset discussed above, there is a 0.1 kJ mole⁻¹ discrepancy between the values shown in Table II for E^C and for the sum of its components $V_{intra} + V_{inter} + E_k$. The quantum correction E^A is obtained by integrating the function $S(\nu) W_g^A(\nu)$ as shown in Eq. (3.54) and Fig. 3. Addition of the kinetic energy (calculated from instantaneous velocities^{102, 118}) to the total potential energy results in conservation of energy to one part in thirty thousand with the 0.25 fs integration step size used. As suggested by Andersen¹¹⁹ we graphed the standard deviation of the total energy versus the square of the time step for several molecular dynamics runs. The resulting nearly linear plot verifies the accuracy of our software and hardware as the Verlet integration algorithm gives an error in total energy in proportion to the square of the integration time step.¹¹⁹ To calculate V_{intra} , we first remove a constant representing the zero point energy contribution from the original WATTS intramolecular potential.⁹⁰

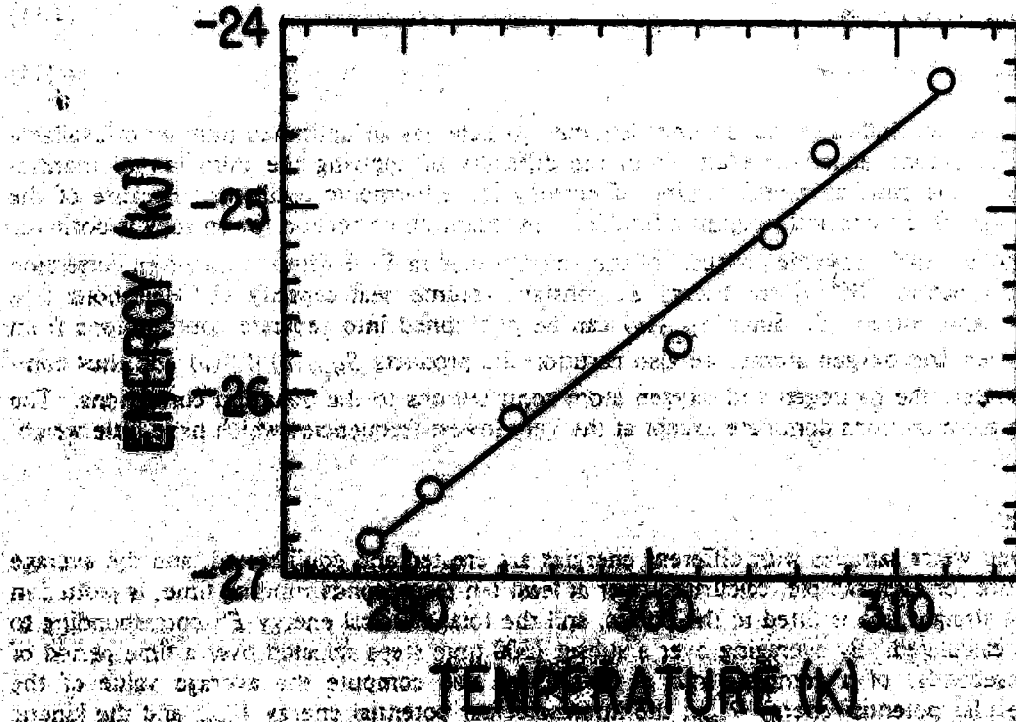


FIG. 7. Calculation of the classical energy E as well as the classical constant volume heat capacity C , by least squares linear fit of E with respect to T . Values of the average temperature T are calculated from the kinetic energy E_k for microcanonical molecular dynamics run of at least 10 picoseconds at each of seven different energies.

TABLE II. Energy (kJ mole⁻¹).

V_{int}	5.2
V_{iner}	-42.1
E_k	11.2
E^C	-25.6 ^a
E^Δ	49.2
$E^{\text{theor}} = E^C + E^\Delta$	23.6
E^{exp}	21.5 ^b

^aCalculated from Fig. 7

^bSee Table IV.

McDonald and Klein⁴⁹ calculate with molecular dynamics an internal potential energy of -33 kJ mole⁻¹ for the WATTS potential for 273 K and 1 gm cm⁻¹ and Reimers and Watts¹⁰¹ report a Monte Carlo calculation giving an internal energy of -29.2 kJ mole⁻¹ for the Watts potential at 298 K and 0.997 gm cm⁻¹. Both calculations differ from the present one in that their water molecules are constrained to be rigid. To determine the effect of this we increased the force constants of our waters first by a factor of four and then sixteen while decreasing the time step first by two and then by four. The result is that the intermolecular potential energy decreases (becomes more negative) with changes on the order of 1 kJ to 2 kJ, indicating that the introduction of flexible waters increases (makes less negative) the intermolecular potential energy over a rigid water calculation. Reimers and Watts run at 298 K and the 1 atm density of 0.997 gm cm⁻¹ compared to our temperature of 300 K and 85 atm density of 1.0 gm cm⁻¹. We performed a special test run at 0.977 gm cm⁻¹ and 298K and calculated an intermolecular potential energy only marginally different from the 1.0 gm cm⁻¹ value, in line with the 0.012 kJ mole⁻¹ shift expected¹⁰⁹ for the total potential energy from experimental thermodynamic measurements. We perform a molecule-by-molecule imaging with force feathering technique following Andersen¹¹¹ rather than potential cut-offs as used by Reimers and Watts or Ewald sums as used by McDonald and Klein. To explore the effects of potential or force smoothing or cutoff, we carried out several additional test runs whose results are summarized in Table III. The standard deviations are given within parentheses and a time step of 0.25 fs is used for each run.

TABLE III. Energies in kJ mole⁻¹ (with standard deviations given in parentheses), as well as bond length and bond angle distortions for several cutoff and feathering boundary methods.

Type	V_{int}	V_{iner}	E^C	$\frac{\delta r}{r_{\text{eq}}} \text{ (%)}$	$\frac{\delta \theta}{\theta_{\text{eq}}} \text{ (%)}$
ANDERSEN	5.2 (0.22)	-42.1 (0.26)	-25.6 (0.00099)	0.52	-1.0
CUTOFF I	5.5 (0.32)	-58.8 (6.1)	-41.8 (6.4)	0.56	-1.0
CUTOFF II	5.5 (0.32)	-50.4 (0.45)	-33.6 (0.029)	0.56	-1.0
AA SMOOTH	27.5	-111.7		1.8	-1.7
IG	4.7			0.2	-0.1

Boundary effects are a significant problem for systems like liquid water where the long range Coulombic forces extend well beyond the dimensions of the model. One way to deal with these nonzero forces near the boundary is to choose a cutoff distance beyond which the potential energy is set to zero. For an atom-atom central force system, this cutoff of the potential can also be done atom by atom (CUTOFF I in Table III), and the resulting forces necessary for molecular dynamics calculations are then the derivatives of the potential within the cutoff distance and zero beyond, with a delta function at the boundary which being of measure zero in

length is never seen by the dynamics calculation. Such energy-force pairs are inconsistent due to the effective neglect of the delta function force term at the cutoff distance which prevents conservation of energy in actual molecular dynamics runs as required for microcanonical systems. The atoms fail to feel the force delta function and can drift back and forth over the cutoff boundary with resulting large potential energy fluctuations. For ordinary Monte Carlo systems where forces are not needed, this difficulty is avoided. We suspect, however, that the large fluctuations in the radial distribution function which occur at the cutoff distance introduce significant perturbations to the system. Table III shows the results of a sample molecular dynamics calculation (CUTOFF I) using a cutoff of 0.875 nm at the midpoint of the 0.85 to 0.90 nm Andersen-Swope feathering which we used for our actual thermodynamic calculations. Notice that the standard deviation (in parentheses) for the intermolecular potential energy is a full fifty-seven percent the kinetic energy.

By cutting off the entire potential molecule-by-molecule⁶⁴ using either the distance between the two centers of mass or the very similar oxygen-oxygen distance as the functional variable, the effectively neglected delta function force terms in molecular dynamics calculations are reduced significantly in magnitude as they now represent truncated dipole-dipole rather than monopole-monopole interactions. Molecule-by-molecule cutoff is also preferable to atom-by-atom cutoff for Monte Carlo calculations as the fluctuations in the radial distribution function at the cutoff distance should be greatly reduced.

One way to conserve energy in molecular dynamics runs while still using the atom-by-atom cutoff method is to set the atom-atom potential beyond the cutoff distance to its value at the cutoff distance (CUTOFF II). The energy-force pair is now consistent and for molecules like water where the forces are essentially Coulombic at the cutoff distance (and the total charge on each molecule is zero) the energy contribution for a molecule-molecule interaction conveniently sums to zero when all the atom-atom interactions are beyond the cutoff distance. The results for this method are also shown in Table III (CUTOFF II). Note the order of magnitude reduction in the standard deviation of the total energy. In both cutoff methods, waters have a tendency to "straddle" the cutoff distance boundary in such a way as to reduce repulsive and increase attractive atom-atom interactions. For CUTOFF II, this has a much smaller effect as the potential energy for any atom-atom interaction changes little across the boundary. For CUTOFF I, however, each atom-atom potential energy function is truncated to zero at the cutoff distance which causes an artificially low average intermolecular potential energy.

Another method which might seem reasonable to try in order to create a consistent energy-force system for molecular dynamics calculations is to smooth each atom-atom potential separately to zero (AA SMOOTH) in some smoothing region and then take the derivative to obtain the force. Indeed such a technique might be useful for systems where the value of the potential at the cutoff distance is near zero. For water this is not the case, however, and AA SMOOTH is totally useless in this application. For our test run we smoothed each potential to zero from 0.85 nm to 0.90 nm, and the corresponding force was calculated. The resulting energy values as shown in Table III differ drastically from the experimental ones due mainly to the large fluctuations in the radial distributions near the cutoff distance. Large forces (20-30 times larger than for the unsmoothed potential) in the smoothing region cause such fluctuations and are a result of the steep slope of the potential necessary to smooth it to zero. One might view this effect as similar to smoothing the neglected delta function force term of the CUTOFF I system over 0.05 nm. Standard deviations are not given for AA SMOOTH because the total energy of the system continued to rise over the course of the run, presumably a consequence of the large forces involved.

The technique by Andersen and Swope (ANDERSEN) which smooths each entire water-water potential to zero may be viewed as smoothing the delta function force terms of a molecule-by-molecule cutoff or equivalently a dipole-dipole interaction over a small range, 0.05 nm in our case. It gives the best energy conservation and smallest V_{mme} and V_{inner} fluctuations as shown in Table III. In addition its waters are put under the least "stress" as measured by V_{mme} .

It may be concluded from the data in Table III that there are several advantages to using the ANDERSEN method. It should also be noted that the choice of method of handling boundary effects significantly influences energy calculations with differences on the order of 10 kJ mole⁻¹.

Table III also contains information on the intramolecular potential energy, the bond lengths, and the bond angles for each system. V_{intra} may be seen as a rough index to the "stress" each water molecule is experiencing. For an ideal gas (IG), i.e. for the same intramolecular potential with the intermolecular potential turned off, the intramolecular potential energy at 300 K is 4.7 kJ mole⁻¹, 0.96 kJ mole⁻¹ above the $(3/2)k_B T$ value of 3.74 kJ mole⁻¹ one would expect if no anharmonic or centrifugal distortion effects were found. In the liquid state each oxygen-hydrogen bond on the average is stretched and each HOH angle on the average is reduced below the equilibrium value, thus increasing V_{intra} above the ideal gas level, which is itself above the harmonic equipartition value.

For a non-rigid calculation at 295.4 K using the LS potential, Rahman, Stillinger, and Lemberg⁷² report $V_{\text{intra}} + V_{\text{inter}} = -34.8$ kJ mole⁻¹, while we calculate for WATTS at 300 K $V_{\text{intra}} + V_{\text{inter}} = -36.9$ kJ mole⁻¹. In their partitioning between V_{intra} and V_{inter} they assume, but do not measure, that V_{intra} is given by the expected undistorted harmonic oscillator values, an approximation which we see to be incorrect, at least in our case, due to anharmonicity, centrifugal distortion, and intermolecular force induced molecular distortion.

The experimental value to which the calculated intermolecular potential energies should be compared deserves some discussion as two significantly different numbers are quoted throughout the literature. One way to obtain the intermolecular potential energy of liquid water is to equate it to the difference in energy of the fluid and vapor states. This is calculated by subtracting PV from the heat of vaporization of water at 300 K. Using this method, Dashevsky and Sarkisov¹⁰⁴ obtain for the intermolecular potential energy from experimental data -41.0 kJ mole⁻¹ at 300 K, and -41.4 kJ mole⁻¹ at 298 K. As pointed out by several workers,^{37, 100, 101, 120-123} however, the bending and stretching frequencies of water change upon condensation, and this difference in intramolecular energy must be accounted for, as well as the correction for conversion of free to hindered translation and rotation. Klemm et al.¹⁰¹ estimate a correction on the order of 7.5 kJ mole⁻¹ which would lead to an intermolecular potential energy of -33.9 kJ mole⁻¹ for 298 K. This may account for the variation in experimental intermolecular potential energy quoted in the literature, as some workers use the corrected value for intermolecular potential energy while others do not. It should also be mentioned that the definitions used of "internal energy" and "internal potential energy" are not always well spelled out or consistent among different authors, making comparisons sometimes difficult and confusing.

The equivalent E^{exp} experimental value for total energy is the difference in energy between liquid water at 300 K and ideal noninteracting water vapor at 0 K with no zero point vibrational energy, measuring energies from the bottom of the potential well for non-interacting molecules. It may be calculated as follows.

$$E_{300 \text{ K}}(\text{liq}) - E_{0 \text{ K}}(\text{vap}) \\ = [E_{300 \text{ K}}(\text{liq}) - E_{0 \text{ K}}(\text{ice})] + [E_{0 \text{ K}}(\text{ice}) - E_{0 \text{ K}}(\text{vap})] \quad (4.13)$$

$$\approx [H_{300 \text{ K}}(\text{liq}) - H_{0 \text{ K}}(\text{ice})] + [H_{0 \text{ K}}(\text{ice}) - H_{0 \text{ K}}(\text{vap})] \quad (4.14)$$

because $E \approx H$ for liquid water and ice. Including the zero point vibrational energy gives the results shown in Table IV.

TABLE IV. Experimental total energy (kJ mole⁻¹).

$H_{300\text{ K}}(\text{liq}) - H_{0\text{ K}}(\text{ice})$	13.4 ^a
$H_{0\text{ K}}(\text{ice}) - H_{0\text{ K}}(\text{vap})$	-47.36 ^b
Vibrational zero point energy	55.45 ^b
E^{exp}	21.5

^aN. Dorsey, *Properties of Ordinary Water Substance*, (Hafner Publishing Co., New York, 1968)

^bD. Eisenberg and W. Kauzman, *The Structure and Properties of Water*, (Oxford University Press, New York, 1969)

Our computed $E^{\text{theor}} = 23.6 \text{ kJ mole}^{-1}$ and experimentally derived $E^{\text{exp}} = 21.5 \text{ kJ mole}^{-1}$ total energies as shown in Tables II and IV thus agree quite well, perhaps better than expected in light of the possible improvements discussed in Section V below.

F. Heat capacity

The energy is fixed in a microcanonical ensemble while the temperature as computed from Eq. (2.6) fluctuates about an average value. Seven distinct water configurations with different energies are created, and the average temperature for each sample is calculated over at least ten picoseconds of running time. The seven points are plotted on the energy-temperature graph in Fig. 7. A straight line is fitted to the points, and the slope is calculated, giving the constant volume heat capacity. The results seen in Table V show quite good agreement with experiment once the quantum correction is added. Note that the calculated value would disagree substantially with experiment if the $11.0 \text{ J deg}^{-1}\text{mole}^{-1}$ intermolecular quantum correction for hindered rotational and translational motion had been omitted.

TABLE V. Constant volume heat capacity (J deg⁻¹mole⁻¹).

C_V^C	106.5
C_V^A	-34.8
$C_V^{\text{theor}} = C_V^C + C_V^A$	71.7
C_V^{exp}	74.5 ^a

^aD. Eisenberg and W. Kauzman, *The Structure and Properties of Water*, (Oxford University Press, New York, 1969)

V. DISCUSSION AND CONCLUSION

The calculations for liquid water presented here are designed to illustrate the quantum correction of classical thermodynamic quantities and not to provide the ultimate in accuracy for those thermodynamic values. Even though the results agree well with experiment, $E^{\text{theor}} = 23.6$ vs $E^{\text{exp}} = 21.5 \text{ kJ mole}^{-1}$, and $C_V^{\text{theor}} = 71.7$ vs $C_V^{\text{exp}} = 74.5 \text{ J deg}^{-1}\text{mole}^{-1}$, it is clear that these classical calculations could be improved. For example, it can be argued that no potential function yet exists for water which is adequate to represent both the inter and intramolecular motions or which is even valid in an effective sense for all phases.^{101, 106} The WATTS potential function which we use in this example calculation is no exception, having been criticized³⁹ on the ground that radial distribution functions calculated from it do not agree with experiment. It is unlikely, as we've seen, to properly account for the change in vibrational frequencies^{10, 37, 120-123} on going from the gas to the liquid phase, as there is no direct coupling between intermolecular distances and the intramolecular part of the potential. The reader is referred to the recent paper by Reimers, Watts, and Klein¹⁰¹ for a comparison among various existing water potentials and a presentation of a revised Watts potential. The potential we have used is clearly only an effective^{39, 71} molecule-molecule potential, as it omits three (and higher)

molecule effects^{35, 76, 92-96, 124, 125} which surely must exist. In addition, one could make a more accurate calculation by including a correction^{6, 16, 37} for the tails of the potential beyond the 0.85 to 0.90 nm region at which we feathered the potential to zero or one could try other long range correction techniques such as Ewald sums.¹²⁶ It seems clear from the large variations in energy among different choices of boundary treatment that much more needs to be learned about the effects of different boundary treatments on systems with long range potentials and their convergence to experimental values. Related questions have been raised by Pangali, Rao, and Berne⁶⁵ with respect to Monte Carlo calculations. The methodology of quantum correction illustrated here would work equally well with any or all of the improvements mentioned above to the classical part of the calculations.

A substantial amount of calculation is needed to achieve the accuracy illustrated in Fig. 7. The long simulation time to achieve a stable average can be interpreted in terms of the unusual "stickiness" of liquid water.^{62, 63} The 95 picoseconds of total molecular simulation time illustrated in Fig. 7 required 190 hours of real time on an array processor.^{107, 108} The array processor speed is approximately 35 times¹⁰⁸ that achieved in optimized Fortran on a DEC VAX 11/780 with a floating point accelerator, and judging from previously reported figures,⁶² 5-10 times faster than a rigid water calculation on an IBM 360/91. Our 2000 time steps per hour when scaled for number of particles and cut-off radius is roughly comparable to the speed reported by Rapaport and Scheraga^{87, 110} for their array processor molecular dynamics calculation for rigid water, taking into account that they use a predictor-corrector integrator, while we only use one force evaluation per time step. The total number of atom-atom force evaluations is 1×10^{11} and the number of calculations of the total force vector on an atom (summed over all its pairwise potential interactions with other atoms) is 1×10^8 . This latter figure might be roughly compared in computational effort to the total number of configurations tried in a similar Monte Carlo calculation, i.e. the number of times an atom is moved and a new potential energy is calculated as a sum over all atomic pairwise interactions with other atoms. Since each molecular dynamics atomic force evaluation delivers the three Cartesian components of the atomic force vector in contrast to the scalar Monte Carlo computation of potential energy, it might be argued that the proper number to compare to an equivalent number of Monte Carlo configuration tries is 3×10^8 . One might also compare the 380 000 time steps to an equivalent number of Monte Carlo passes through all variables. It has been argued by Rao, Pangali, and Berne⁶² that one Monte Carlo pass for rigid water can be compared in computational effort to one molecular dynamic time step, but for problems accessible to Monte Carlo solution that Monte Carlo may be several times more efficient in terms of distance moved per pass versus per molecular dynamics time step.

A very different way to compute dynamics and thermodynamic quantities which may in time become practical would be a quantum force classical trajectory approach¹²⁷ in which at each time step in the classical trajectory the forces (for the dynamics) and the energy (for the thermodynamics) are computed from *ab initio* quantum mechanics.

It is clear from these results that one can and should take into account quantum corrections in testing molecular potential energy functions against experimental thermodynamic measurements. In particular, the intermolecular (hindered translational and rotational) motions in strongly associated liquids can lead to significant errors if the related quantum corrections are neglected in thermodynamic comparisons with experiment. Consider, for example, that the intermolecular quantum correction to energy for our system is 38 percent of the kinetic energy while the intermolecular quantum correction to free energy is 20 percent of the kinetic energy. The intermolecular quantum correction to heat capacity is 15 percent of the experimental value while the intermolecular quantum correction for entropy is 10 percent of the experimental value.¹⁰⁹ Similarly, motions in polymers (which can themselves be affected by solvent interactions) may also need thermodynamic quantum correction, and the molecular dynamics method illustrated here also can be applied in such cases.

An interesting aspect of this quantum correction technique is that after the dynamics (which in general depend upon all the atoms) are computed, the quantum corrections may be

calculated atom by atom, and thus the quantum effects on the thermodynamic variables may be considered separately for different elements, different chemical environments of the same element, different types of molecules, or molecules in different environments. An advantage of the basically classical molecular dynamics approach to thermodynamics presented here is the ability to visualize and understand intuitively the classical motions and frequencies responsible for thermodynamic effects. For example, one can understand in a very pictorial way the dominance of the water quantum corrections by the hydrogen atom motions as illustrated in Figs. 3-6.

This technique for quantum correcting classical thermodynamic quantities should be applicable to a wide variety of molecular systems including polymers such as proteins and nucleic acids, liquids, solutions and solids. For example the molecular dynamics method could be used to compute and quantum correct the heat capacity of biomolecules in solution, a quantity known to depend on molecular conformation. Thermodynamic calculations can be made involving both intermolecular and intramolecular degrees of freedom. In addition, this approach can be extended to treat quasiequilibrium cases, such as the calculation of thermodynamic quantities as a function of progress along a chemical reaction coordinate or thermodynamic quantities for molecules in special surroundings such as boundary waters near a protein.

ACKNOWLEDGEMENTS

We thank William C. Swope and Hans C. Andersen for many helpful discussions and the use of their array processor water intermolecular force calculation software and the Office of Naval Research, Chemistry, the National Science Foundation, Chemistry, and the National Institutes of Health, both General Medical Sciences and Division of Research Resources, for providing the support which has made this work possible.

1. D. A. McQuarrie, *Statistical Mechanics*, Harper and Row, New York (1976).
2. H. C. Andersen, "Molecular dynamics simulations at constant pressure and/or temperature," *J. Chem. Phys.*, vol. 72, p. 2384 (1980).
3. J. L. Lebowitz, J. K. Percus, and L. Verlet, "Ensemble dependence of fluctuations with application to machine computations," *Phys. Rev.*, vol. 153, p. 250 (1967).
4. P. S. Y. Cheung, "On the calculation of specific heats, thermal pressure coefficients and compressibilities in molecular dynamics simulations," *Mol. Phys.*, vol. 33, p. 519 (1977).
5. J. G. Kirkwood, "Statistical mechanics of fluid mixtures," *J. Chem. Phys.*, vol. 3, p. 300 (1935).
6. J. A. Barker and D. Henderson, "What is liquid? Understanding the states of matter," *Rev. Mod. Phys.*, vol. 48, p. 587 (1976).
7. M. Mezei, S. Swaminathan, and D. L. Beveridge, "Ab initio calculation of the free energy of liquid water," *J. Am. Chem. Soc.*, vol. 100, p. 3255 (1978).
8. M. Mezei, "Excess free energy of different water models computed by Monte Carlo methods," *Mol. Phys.* (1982). In press.
9. R. J. Harrison, J. A. Cox, G. H. Bishop, and S. Yip, "Computation of entropy in grain boundary computer simulations," in *Computer Simulation for Materials Application*, ed. R. J. Arsenault, J. R. Beales, and J. A. Simmons, p. 604, NBS Nuclear Metallurgy Series Vol. 20 (1976).
10. D. Eisenberg and W. Kauzmann, *The Structure and Properties of Water*, Oxford University Press, New York (1969).

11. E. Wigner, "On the quantum correction for thermodynamic equilibrium." *Phys. Rev.*, vol. 40, p. 749 (1932).
12. J. G. Kirkwood, "Quantum statistics of almost classical assemblies." *Phys. Rev.*, vol. 44, p. 31 (1933).
13. J. G. Kirkwood, "Statistical theory of low frequency intermolecular forces." *J. Chem. Phys.*, vol. 1, p. 597 (1933).
14. H. S. Green, "The quantum mechanics of assemblies of interacting particles." *J. Chem. Phys.*, vol. 19, p. 955 (1951).
15. J.-P. Hansen and J.-J. Weis, "Quantum corrections to the coexistence curve of neon near the triple point." *Phys. Rev.*, vol. 188, p. 314 (1969).
16. J. A. Barker, R. A. Fisher, and R. O. Watts, "Liquid argon: Monte Carlo and molecular dynamics calculations." *Mol. Phys.*, vol. 21, p. 657 (1971).
17. E. J. Derderian and W. A. Steele, "Expansion for the quantum second virial coefficient using hard-sphere basis functions." *J. Chem. Phys.*, vol. 55, p. 5795 (1971).
18. Y. Singh and J. Ram, "On the quantum corrections to the radial distribution function and to the thermodynamic properties of fluids." *Mol. Phys.*, vol. 25, p. 145 (1973).
19. H. L. Lemberg and F. H. Stillinger, "Central-force model for liquid water." *J. Chem. Phys.*, vol. 62, p. 1677 (1975).
20. J. G. Powles and G. Rickayzen, "Quantum corrections and the computer simulation of molecular fluids." *Mol. Phys.*, vol. 38, p. 1875 (1979).
21. E. D. Glandt, "Quantum corrections to the thermodynamic properties of absorbed fluid phases." *J. Chem. Phys.*, vol. 74, p. 1321 (1981).
22. H. Fredrikze, "Comment on 'Quantum corrections and the computer simulation of molecular fluids'." *Mol. Phys.*, vol. 43, p. 489 (1981).
23. P. C. Hemmer, "The hard core quantum gas at high temperatures." *Phys. Lett.*, vol. 27A, p. 377 (1968).
24. B. Jancovici, "Quantum-mechanical equation of state of a hard-sphere gas at high temperature." *Phys. Rev.*, vol. 178, p. 295 (1969).
25. B. Jancovici, "Quantum-mechanical equation of state of a hard-sphere gas at high temperature. II." *Phys. Rev.*, vol. 184, p. 119 (1969).
26. W. G. Gibson, "Quantum corrections to the equation of state for nonanalytic potentials." *Phys. Rev. A*, vol. 5, p. 862 (1972).
27. W. G. Gibson, "Quantum corrections to the properties of a dense fluid with non-analytic intermolecular potential function I. The general case." *Mol. Phys.*, vol. 30, p. 1 (1975).
28. W. G. Gibson, "Quantum corrections to the properties of a dense fluid with non-analytic intermolecular potential function II. Hard spheres." *Mol. Phys.*, vol. 30, p. 13 (1975).
29. B. P. Singh and S. K. Sinha, "Quantum corrections to the equilibrium properties of dense fluids: Application to hard-sphere fluids." *J. Chem. Phys.*, vol. 67, p. 3645 (1977).
30. B. P. Singh and S. K. Sinha, "Quantum corrections to the equation of state of a fluid using hard-sphere basis functions." *J. Chem. Phys.*, vol. 68, p. 562 (1978).
31. B. P. Singh and S. K. Sinha, "Quantum corrections to the thermodynamic properties of the hard-sphere fluid." *J. Chem. Phys.*, vol. 69, p. 2927 (1978).
32. B. P. Singh and S. K. Sinha, "Quantum corrections to the equilibrium properties of a dense fluid with square-well plus hard-core potential." *J. Chem. Phys.*, vol. 70, p. 552 (1979).

33. J. D. Doll and L. E. Myers, "Semiclassical Monte Carlo methods," *J. Chem. Phys.*, vol. 71, p. 2880 (1979).
34. R. P. Feynman and A. R. Hibbs, *Quantum Mechanics and Path Integrals*, McGraw-Hill, New York (1965).
35. F. Stillinger, "Theory and molecular models for water," *Adv. Chem. Phys.*, vol. 31, p. 1 (1975).
36. G. E. Uhlenbeck and L. Gropper, "The equation of state of a non-ideal Einstein-Bose or Fermi-Dirac gas," *Phys. Rev.*, vol. 41, p. 79 (1932).
37. J. C. Owicki and H. A. Scheraga, "Monte Carlo calculations in the isothermal isobaric ensemble I. Liquid water," *J. Am. Chem Soc.*, vol. 99, p. 7403 (1977).
38. P. H. Berens and K. R. Wilson, "Molecular dynamics and spectra: I. Diatomic rotation and vibration," *J. Chem. Phys.*, vol. 74, p. 4872 (1981).
39. P. H. Berens, S. R. White, and K. R. Wilson, "Molecular dynamics and spectra: II. Diatomic Raman," *J. Chem. Phys.*, vol. 75, p. 515 (1981).
40. E. O. Brigham, *The Fast Fourier Transform*, Prentice-Hall, Englewood Cliffs, New Jersey (1974).
41. W. Marshall and S. W. Lovesey, *Theory of Thermal Neutron Scattering*, Oxford University Press, London (1971).
42. K. R. Symon, *Mechanics*, Addison-Wesley, Reading, Massachusetts (1964).
43. F. G. Stremler, *Introduction to Communication Systems*, Addison-Wesley, Reading, Massachusetts (1977).
44. P. Barnes, "Machine simulation of water," in *Progress in Liquid Physics*, ed. C. A. Croxton, p. 391, John Wiley, Chichester (1978).
45. D. W. Wood, "Computer simulation of water and aqueous solutions," in *Water, A Comprehensive Treatise, Vol. 6, Recent Advances*, ed. F. Franks, p. 279, Plenum, New York (1979).
46. D. L. Beveridge, M. Mazei, P. K. Mehrotra, R. T. Marchese, G. R.-S. T. Vasu, and S. Swaminathan, "Monte Carlo computer simulation studies of the equilibrium properties and structure of liquid water," in *Molecular-Based Study and Prediction of Fluid Properties*, *Adv. Chem. Ser.*, ed. J. M. Halle and G. A. Mansoori, American Chemical Society, Washington, D.C. (1982). To be published.
47. S. P. Goel and R. W. Hockney, "A resource letter CSSMD-1: Computer simulation studies by the method of molecular dynamics," *Rev. Bras. Fis.*, vol. 4, p. 121 (1974).
48. J. D. Bernal and R. H. Fowler, "A theory of water and ionic solution, with particular reference to hydrogen and hydroxyl ions," *J. Chem. Phys.*, vol. 1, p. 515 (1933).
49. J. S. Rowlinson, "The lattice energy of ice and the second virial coefficient of water vapour," *Trans. Faraday Soc.*, vol. 47, p. 120 (1951).
50. J. A. Barker and R. O. Watts, "Structure of water: A Monte Carlo calculation," *Chem. Phys. Lett.*, vol. 3, p. 144 (1969).
51. J. A. Barker and R. O. Watts, "Monte Carlo studies of the dielectric properties of water-like models," *Mol. Phys.*, vol. 26, p. 789 (1973).
52. R. O. Watts, "Monte Carlo studies of liquid water," *Mol. Phys.*, vol. 28, p. 1069 (1974).
53. A. Ben-Naim and F. H. Stillinger, "Aspects of the statistical mechanical theory of water," in *Structure and Transport Processes in Water and Aqueous Solutions*, ed. R. A. Horne, Wiley-Interscience, New York (1972).

54. A. Rahman and F. H. Stillinger, "Molecular dynamics study of liquid water," *J. Chem. Phys.*, vol. 55, p. 3336 (1971).
55. F. H. Stillinger and A. Rahman, "Molecular dynamics study of temperature effects on water structure and kinetics," *J. Chem. Phys.*, vol. 57, p. 1281 (1972).
56. F. H. Stillinger and H. L. Lemberg, "Symmetry breaking in water molecule interactions," *J. Chem. Phys.*, vol. 62, p. 1340 (1975).
57. F. H. Stillinger and A. Rahman, "Improved simulation of liquid water by molecular dynamics," *J. Chem. Phys.*, vol. 60, p. 1545 (1974).
58. F. H. Stillinger and A. Rahman, "Molecular dynamics calculation of neutron inelastic scattering from water," in *Molecular Motions in Liquids*, ed. J. Lascombe, p. 478, D. Reidel, Dordrecht-Holland (1974).
59. A. Rahman and F. H. Stillinger, "Propagation of sound in water. A molecular dynamics study," *Phys. Rev. A*, vol. 10, p. 368 (1974).
60. F. H. Stillinger and A. Rahman, "Molecular dynamics study of liquid water under high compression," *J. Chem. Phys.*, vol. 61, p. 4973 (1974).
61. W. F. van Gunsteren, H. J. C. Berendsen, and J. A. C. Rullmann, "Inclusion of reaction fields in molecular dynamics: Application to liquid water," *Faraday Discuss. Chem. Soc.*, vol. 66, p. 58 (1978).
62. M. Rao, C. Pangali, and B. J. Berne, "On the force bias Monte Carlo simulation of water: methodology, optimization and comparison with molecular dynamics," *Mol. Phys.*, vol. 37, p. 1773 (1979).
63. M. Mezei, S. Swaminathan, and D. L. Beveridge, "Convergence characteristics of Monte Carlo-Metropolis computer simulations on liquid water," *J. Chem. Phys.*, vol. 71, p. 3366 (1979).
64. M. Mezei, "Estimation of the difference between molecular dynamics and Monte Carlo averages due to the truncation of the potential," *Chem. Phys. Lett.*, vol. 74, p. 105 (1980).
65. C. Pangali, M. Rao, and B. J. Berne, "A Monte Carlo study of structural and thermodynamic properties of water: dependence on the system size and on the boundary conditions," *Mol. Phys.*, vol. 40, p. 661 (1980).
66. A. Geiger, A. Rahman, and F. H. Stillinger, "Molecular dynamics study of the hydration of Lennard-Jones solutes," *J. Chem. Phys.*, vol. 70, p. 263 (1979).
67. M. Mezei and D. L. Beveridge, "Further quasicomponent distribution function analysis of liquid water. Temperature dependence of the results," *J. Chem. Phys.*, vol. 76, p. 593 (1982).
68. L. L. Shipman and H. A. Scheraga, "An empirical intermolecular potential energy function for water," *J. Phys. Chem.*, vol. 78, p. 909 (1974).
69. L. L. Shipman, J. C. Owicki, and H. A. Scheraga, "Structure, energetics, and dynamics of the water dimer," *J. Phys. Chem.*, vol. 78, p. 2055 (1974).
70. L. L. Shipman and H. A. Scheraga, "Computation of the intermolecular vibrational modes of a tetrahedral water pentamer at the core of an ice-like water cluster," *J. Phys. Chem.*, vol. 79, p. 380 (1975).
71. F. Stillinger, "Effective pair interactions in liquids. Water," *J. Phys. Chem.*, vol. 74, p. 3677 (1970).
72. A. Rahman, F. H. Stillinger, and H. L. Lemberg, "Study of a central force model for liquid water by molecular dynamics," *J. Chem. Phys.*, vol. 63, p. 5223 (1975).
73. F. Stillinger and A. Rahman, "Revised central force potentials for water," *J. Chem. Phys.*, vol. 68, p. 666 (1978).

74. H. Popkie, H. Kistenmacher, and E. Clementi, "Study of the structure of molecular complexes. IV. The Hartree-Fock potential for the water dimer and its application to the liquid state," *J. Chem. Phys.*, vol. 59, p. 1325 (1973).
75. H. Kistenmacher, H. Popkie, E. Clementi, and R. O. Watts, "Study of the structure of molecular complexes. VII. Effect of correlation energy corrections to the Hartree-Fock water-water potential on Monte Carlo simulations of liquid water," *J. Chem. Phys.*, vol. 60, p. 4455 (1974).
76. H. Kistenmacher, G. C. Lie, H. Popkie, and E. Clementi, "Study of the structure of molecular complexes. VI. Dimers and small clusters of water molecules in the Hartree-Fock approximation," *J. Chem. Phys.*, vol. 61, p. 546 (1974).
77. D. J. Evans and R. O. Watts, "Water-water pair interactions and the second virial coefficient of steam," *Mol. Phys.*, vol. 28, p. 1233 (1974).
78. G. C. Lie and E. Clementi, "Study of the structure of molecular complexes. XII. Structure of liquid water obtained by Monte Carlo simulation with the Hartree-Fock potential corrected by inclusion of dispersion forces," *J. Chem. Phys.*, vol. 62, p. 2195 (1975).
79. R. O. Watts, "The effect of ion pairs on water structure," *Mol. Phys.*, vol. 32, p. 659 (1976).
80. E. Clementi, *Determination of Liquid Water Structure. Coordination Numbers for Ions and Solvation for Biological Molecules*, Springer-Verlag, Berlin (1976).
81. O. Matsuoka, M. Yoshimine, and E. Clementi, "CI study of the water dimer potential surface," *J. Chem. Phys.*, vol. 64, p. 1351 (1976).
82. G. C. Lie, E. Clementi, and M. Yoshimine, "Study of the structure of molecular complexes. XIII. Monte Carlo simulation of liquid water with a configuration interaction pair potential," *J. Chem. Phys.*, vol. 64, p. 2314 (1976).
83. G. C. Lie and E. Clementi, "Calculation of the second virial coefficients for water using a recent ab initio potential," *J. Chem. Phys.*, vol. 64, p. 5308 (1976).
84. D. L. Beveridge, M. Mezzi, S. Swaminathan, and S. W. Harrison, "Monte Carlo studies of the structure of liquid water and dilute aqueous solutions," in *Computer Simulation of Bulk Matter from a Molecular Perspective*, ed. P. G. Lykos, American Chemical Society, Washington (1978).
85. S. F. O'Shea and P. R. Tremaine, "Thermodynamics of liquid and supercritical water at 900 C by a Monte-Carlo Method," *J. Chem. Phys.*, vol. 84, p. 3304 (1980).
86. R. W. Impey, M. L. Klein, and I. R. McDonald, "Molecular dynamics studies of the structure of water at high temperatures and densities," *J. Chem. Phys.*, vol. 74, p. 647 (1981).
87. D. C. Rapoport and H. A. Scheraga, "Structure and dynamics of the configuration interaction model of liquid water," *Chem. Phys. Lett.*, vol. 78, p. 491 (1981).
88. S. Swaminathan and D. L. Beveridge, "A theoretical study of the structure of liquid water based on quasi-component distribution functions," *J. Am. Chem. Soc.*, vol. 99, p. 8392 (1977).
89. I. R. McDonald and M. Klein, "Intermolecular potentials and the simulation of liquid water," *J. Chem. Phys.*, vol. 68, p. 4875 (1978).
90. R. O. Watts, "An accurate potential for deformable water molecules," *Chem. Phys.*, vol. 26, p. 367 (1977).
91. I. McDonald and M. Klein, "Molecular dynamics studies of hydrogen-bonded liquids," *Faraday Discuss. Chem. Soc.*, vol. 66, p. 48 (1978).

92. F. H. Stillinger and C. W. David, "Polarization model for water and its ionic dissociation products," *J. Chem. Phys.*, vol. 69, p. 1473 (1978).
93. F. H. Stillinger, "Dynamics and ensemble averages for the polarization models of molecular interactions," *J. Chem. Phys.*, vol. 71, p. 1647 (1979).
94. P. Barnes, J. L. Finney, J. D. Nicholas, and J. E. Quinn, "Cooperative effects in simulated water," *Nature*, vol. 282, p. 459 (1979).
95. J. M. Goodfellow, J. L. Finney, and P. Barnes, "Monte Carlo computer simulation of water-amino acid interactions," *Proc. R. Soc. London, Ser B*, vol. 214, p. 213 (1982).
96. J. M. Goodfellow, "Cooperative effects in water-biomolecule crystal systems," *Proc. Natl. Acad. Sci. USA*, vol. 79, p. 4977 (1982).
97. R. A. Nemenoff, J. Snir, and H. A. Scheraga, "A revised empirical potential for conformational, intermolecular, and solvation studies. 5. Development and testing of parameters for amides, amino acids, and peptides," *J. Phys. Chem.*, vol. 82, p. 2527 (1978).
98. F. T. Marchese, P. K. Mehrotra, and D. L. Beveridge, "A revised potential function for the water dimer in the EPEN/2 form," *J. Phys. Chem.*, vol. 85, p. 1 (1981).
99. H. J. C. Berendsen, J. P. M. Postma, W. F. van Gunsteren, and J. Hermans, "Interaction models for water in relation to protein hydration," in *Intermolecular Forces*, ed. B. Pullman, p. 331, D. Reidel Publishing Co., Dordrecht, Holland (1981).
100. W. L. Jorgensen, *J. Chem. Phys.* (1982). Submitted.
101. J. R. Reimers, R. O. Watts, and M. L. Klein, "Intermolecular potential functions and the properties of water," *Chem. Phys.*, vol. 64, p. 95 (1982).
102. W. C. Swope, H. C. Andersen, P. H. Berens, and K. R. Wilson, "A computer simulation method for the calculation of equilibrium constants for the formation of physical clusters of molecules: Application to small water clusters," *J. Chem. Phys.*, vol. 76, p. 637 (1982).
103. G. N. Sarkisov, V. G. Dashevsky, and G. G. Malenkov, "The thermodynamics and structure of liquid water: The Monte Carlo method," *Mol. Phys.*, vol. 27, p. 1249 (1974).
104. V. G. Dashevsky and G. N. Sarkisov, "The solvation and hydrophobic interaction of non-polar molecules in water in the approximation of interatomic potentials: The Monte Carlo method," *Mol. Phys.*, vol. 27, p. 1271 (1974).
105. O. Weret and S. A. Rice, "A new model for liquid water," *J. Amer. Chem. Soc.*, vol. 94, p. 8983 (1972).
106. M. D. Morse and S. A. Rice, "Tests of effective pair potentials for water: Predicted ice structures," *J. Chem. Phys.*, vol. 76, p. 650 (1982).
107. K. R. Wilson, "Many-atom molecular dynamics with an array processor," in *Minicomputers and Large Scale Computations*, ed. P. Lykos, p. 147, American Chemical Society, Washington (1977).
108. P.H. Berens and K.R. Wilson, "Molecular dynamics with an array processor," *J. Comp. Chem.* (1982). Submitted.
109. N. Dorsey, *Properties of Ordinary Water Substance*, Hafner Publishing Co., New York (1968).
110. D. C. Rapaport and H. A. Scheraga, "Hydration of inert solutes. A molecular dynamics study," *J. Chem. Phys.*, vol. 86, p. 873 (1982).
111. T. Andrea, W. C. Swope, and H. C. Andersen. To be submitted.
112. R. K. Otnes and L. Enochson, *Applied Time Series Analysis. Vol. I: Basic Techniques*, Wiley-Interscience, New York (1978).

113. S. Califano, *Vibrational States*, Wiley, London (1976).
114. G. Herzberg, *Molecular Spectra and Molecular Structure, II. Infrared and Raman Spectra of Polyatomic Molecules*, Van Nostrand, Princeton, New Jersey (1945).
115. G. E. Walrafen, "Raman and infrared spectral investigations of water structure," in *Water, A Comprehensive Treatise, Vol. I, The Physics and Chemistry of Water*, ed. F. Franks, p. 151, Plenum, New York (1972).
116. R. Mills, "Self-diffusion in normal and heavy water in the range 1-45C," *J. Phys. Chem.*, vol. 77, p. 685 (1973).
117. K. Krynicki, C. D. Green, and D. W. Sawyer, "Pressure and temperature dependence of self-diffusion in water," *Faraday Discuss. Chem. Soc.*, vol. 66, p. 199 (1978).
118. D. Beeman, "Some multistep methods for use in molecular dynamics calculations," *J. Comput. Phys.*, vol. 20, p. 130 (1976).
119. H. C. Anderson. Private communication.
120. M. G. Scalet, M. Stavola, and S. A. Rice, "A zeroth order random network model of liquid water," *J. Chem. Phys.*, vol. 70, p. 3927 (1979).
121. M. G. Scalet and S. A. Rice, "The water-water pair potential near the hydrogen bonded equilibrium configuration," *J. Chem. Phys.*, vol. 72, p. 3236 (1980).
122. M. G. Scalet and S. A. Rice, "The enthalpy and heat capacity of liquid water and the ice polymorphs from a random network model," *J. Chem. Phys.*, vol. 72, p. 3248 (1980).
123. M. G. Scalet and S. A. Rice, "The entropy of liquid water from the random network model," *J. Chem. Phys.*, vol. 72, p. 3260 (1980).
124. E. Clementi, W. Kolos, G. C. Lie, and G. Ranghino, "Nonadditivity of interaction in water trimers," *Int. J. Quantum Chem.*, vol. 17, p. 377 (1980).
125. D. Hankins, J. W. Moskowitz, and F. H. Stillinger, "Water molecule interactions," *J. Chem. Phys.*, vol. 53, p. 4544 (1970).
126. J. P. Valleau and S. G. Whittington, "A guide to Monte Carlo for statistical mechanics," in *Statistical Mechanics Part A: Equilibrium Techniques*, ed. B. J. Berne, Plenum, New York (1977).
127. D. Fredkin, A. Komornicki, S. R. White, and K. R. Wilson, "Ab initio infrared and raman spectra," *J. Chem. Phys.* (1982). In press.

TECHNICAL REPORT DISTRIBUTION LIST, GEN

<u>No.</u> <u>Copies</u>		<u>No.</u> <u>Copies</u>		
	Office of Naval Research Attn: Code 472 800 North Quincy Street Arlington, Virginia 22217	2	U.S. Army Research Office Attn: CRD-AA-IP P.O. Box 1211 Research Triangle Park, N.C. 27709	1
	ONR Western Regional Office Attn: Dr. R. J. Marcus 1030 East Green Street Pasadena, California 91106	1	Naval Ocean Systems Center Attn: Mr. Joe McCartney San Diego, California 92152	1
	ONR Eastern Regional Office Attn: Dr. L. H. Peebles Building 114, Section D 666 Summer Street Boston, Massachusetts 02210	1	Naval Weapons Center Attn: Dr. A. B. Amster, Chemistry Division China Lake, California 93555	1
	Director, Naval Research Laboratory Attn: Code 6100 Washington, D.C. 20390	1	Naval Civil Engineering Laboratory Attn: Dr. R. W. Drisko Port Hueneme, California 93401	1
	The Assistant Secretary of the Navy (RE&S) Department of the Navy Room 4E736, Pentagon Washington, D.C. 20390	1	Department of Physics & Chemistry Naval Postgraduate School Monterey, California 93940	1
	Commander, Naval Air Systems Command Attn: Code 310C (H. Rosenwasser) Department of the Navy Washington, D.C. 20360	1	Scientific Advisor Commandant of the Marine Corps (Code RD-1) Washington, D.C. 20380	1
12	Defense Technical Information Center Building 5, Cameron Station Alexandria, Virginia 22314		Naval Ship Research and Development Center Attn: Dr. G. Bosmajian, Applied Chemistry Division Annapolis, Maryland 21401	1
1	Dr. Fred Saalfeld Chemistry Division, Code 6100 Naval Research Laboratory Washington, D.C. 20375		Naval Ocean Systems Center Attn: Dr. S. Yamamoto, Marine Sciences Division San Diego, California 91232	1
		1	Mr. John Boyle Materials Branch Naval Ship Engineering Center Philadelphia, Pennsylvania 19112	1

SP472-3/A3

472:GAN:716:enj
78u472-608

TECHNICAL REPORT DISTRIBUTION LIST, GEN

	<u>No.</u> <u>Copies</u>
Mr. James Kelley DTNSADC Code 2803 Annapolis, Maryland 21402	1
Mr. A. M. Ansalone Administrative Librarian PLASTEC/ARRADCOM Bldg 3401 Dover, New Jersey 07801	1

TECHNICAL REPORT DISTRIBUTION LIST, 051A

	<u>No.</u> <u>Copies</u>		<u>No.</u> <u>Copies</u>
Dr. M. A. El-Sayed University of California, Los Angeles Department of Chemistry Los Angeles, California 90024	5 st	Dr. M. Rauhut American Cyanamid Company Chemical Research Division Bound Brook, New Jersey 08805	1
Dr. M. W. Windsor Washington State University Department of Chemistry Pullman, Washington 99163	1	Dr. J. I. Zink University of California, Los Angeles Department of Chemistry Los Angeles, California 90024	1
Dr. E. R. Bernstein Colorado State University Department of Chemistry Fort Collins, Colorado 80521	1	Dr. B. Schechtman IBM San Jose Research Center 5600 Cottle Road San Jose, California 95143	1
Dr. C. A. Heller Naval Weapons Center Code 6059 China Lake, California 93555	1	Dr. John Cooper Code 6130 Naval Research Laboratory Washington, D.C. 20375	1
Dr. J. R. MacDonald Naval Research Laboratory Chemistry Division Code 6110 Washington, D.C. 20375	1		
Dr. G. B. Schuster University of Illinois Chemistry Department Urbana, Illinois 61801	1		
Dr. E. M. Eyring University of Utah Department of Chemistry Salt Lake City, Utah 84112	1		
Dr. A. Adamson University of Southern California Department of Chemistry Los Angeles, California 90007	1		
Dr. V. S. Wrighton Massachusetts Institute of Technology Department of Chemistry Cambridge, Massachusetts 02139	1		

TECHNICAL REPORT DISTRIBUTION LIST, 0512

<u>No.</u> <u>Copies</u>	<u>No.</u> <u>Copies</u>		
Professor K. Wilson Department of Chemistry, B-014 University of California, San Diego La Jolla, California 92093	1	Dr. B. Vonnegut State University of New York Earth Sciences Building 1400 Washington Avenue Albany, New York 12203	1
Professor C. A. Ansell Department of Chemistry Purdue University West Lafayette, Indiana 47907	1	Dr. Hank Looz Laguna Research Laboratory 21421 Stans Lane Laguna Beach, California 92651	1
Professor P. Meijer Department of Physics Catholic University of America Washington, D.C. 20064	1	Dr. John Latham University of Manchester Institute of Science & Technology P.O. Box 88 Manchester, England M501QD	1
Dr. S. Greer Chemistry Department University of Maryland College Park, Maryland 20742	1		
Professor P. Delashay New York University 100 Washington Square East New York, New York 10003	1		
Dr. T. Ashworth Department of Physics South Dakota School of Mines & Technology Rapid City, South Dakota 57701	1		
Dr. G. Gross New Mexico Institute of Mining & Technology Socorro, New Mexico 87801	1		
Dr. J. Kassner Space Science Research Center University of Missouri - Rolla Rolla, Missouri 65401	1		
Dr. J. Telford University of Nevada System Desert Research Institute Lab of Atmospheric Physics Reno, Nevada 89507	1		

TECHNICAL REPORT DISTRIBUTION LIST, 051C

<u>No.</u> <u>Copies</u>		<u>No.</u> <u>Copies</u>		
	Dr. H. B. Denton Department of Chemistry University of Arizona Tucson, Arizona 85721	1	Dr. John Duffin United States Naval Postgraduate School Monterey, California 93940	1
	Dr. R. A. Osteryoung Department of Chemistry State University of New York at Buffalo Buffalo, New York 14214	1	Dr. G. M. Hieftje Department of Chemistry Indiana University Bloomington, Indiana 47401	1
	Dr. B. R. Kovalski Department of Chemistry University of Washington Seattle, Washington 98105	1	Dr. Victor L. Rehn Naval Weapons Center Code 3813 China Lake, California 93555	1
	Dr. S. P. Perone Department of Chemistry Purdue University Lafayette, Indiana 47907	1	Dr. Christie G. Enke Michigan State University Department of Chemistry East Lansing, Michigan 48824	1
	Dr. D. L. Venezky Naval Research Laboratory Code 6130 Washington, D.C. 20375	1	Dr. Kent Eisentraut, MFT Air Force Materials Laboratory Wright-Patterson AFB, Ohio 45433	1
	Dr. H. Freiser Department of Chemistry University of Arizona Tucson, Arizona 85721	1	Walter G. Cox, Code 3632 Naval Underwater Systems Center Building 148 Newport, Rhode Island 02840	1
	Dr. Fred Saalfeld Naval Research Laboratory Code 6110 Washington, D.C. 20375	1	Professor Isiah N. Warner Texas A&M University Department of Chemistry College Station, Texas 77840	1
	Dr. H. Chernoff Department of Mathematics Massachusetts Institute of Technology Cambridge, Massachusetts 02139	1	Professor George R. Morrison Cornell University Department of Chemistry Ithaca, New York 14853	1
	Dr. K. Wilson Department of Chemistry University of California, San Diego La Jolla, California	1	Professor J. Janata Department of Bioengineering University of Utah Salt Lake City, Utah 84112	1
	Dr. A. Zirino Naval Undersea Center San Diego, California 92132	1	Dr. Carl Heil Naval Weapons Center China Lake, California 93555	1

472:GAN:716:lab
78u472-608

TECHNICAL REPORT DISTRIBUTION LIST, 051C

No.
Copies

Dr. L. Jarvis
Code 6100
Naval Research Laboratory
Washington, D.C. 20375

1

SECURITY CLASSIFICATION OF THIS PAGE (When Data Entered)